Use of geosynthetics to mitigate problems associated with expansive clay subgrades

J. G. Zornberg[1] and G. H. Roodi[2]

[1] *Priddy Centennial Professor, Department of Civil, Architectural, and Environmental Engineering, University of Texas at Austin, Austin, TX 78712, USA, E-mail: zornberg@mail.utexas.edu (corresponding author)*
[2] *Postdoctoral Fellow, Department of Civil, Architectural, and Environmental Engineering, University of Texas at Austin, Austin, TX 78712, USA. E-mail: hroodi@utexas.edu*

Received 15 November 2019, revised 01 June 2020, accepted 25 August 2020, published 28 May 2021

ABSTRACT: Geosynthetics have recently been used for base course stabilization of roadways subjected to environmental loads associated with the presence of expansive clay subgrades. Repeated cycles of wet and dry seasons have often led to significant, non-uniform moisture changes within clay subgrades, resulting in differential settlements between the roadway edges and its centerline and, ultimately, in environmental longitudinal cracks. This paper quantifies the field performance of different sites in order to assess the effectiveness of using geosynthetics to stabilize the base course of roadways constructed on expansive clay subgrades. This includes evaluation of five full-scale field projects that had been subjected to actual traffic and environmental loads. The long-term performance of geosynthetic-stabilized and control sections was evaluated by quantifying the development and extent of longitudinal cracks and the degradation of the base course stiffness. Collectively, the performance evaluation of the multiple geosynthetic-stabilized and control sections in the five case studies demonstrates that geosynthetics can effectively mitigate roadway problems associated with expansive clay subgrades. In addition, field performance data also indicates that unconfined stiffness and tensile strength may not be sufficient for proper geosynthetic selection, pointing to the need for selecting them using properties that also quantify the soil-geosynthetic interaction.

KEYWORDS: Geosynthetics, Geogrid, Geotextile, Expansive Clay, Base Stabilization, Field Evaluation

REFERENCE: Zornberg, J. G. and Roodi, G. H. (2021). Use of geosynthetics to mitigate problems associated with expansive clay subgrades. *Geosynthetics International*, **28**, No. 3, 279–302. [https://doi.org/10.1680/jgein.20.00043]

1. INTRODUCTION

Over the past few decades, applications involving the use of geosynthetics in roadway systems have become increasingly diverse. This includes their use to stabilize the base course or the subgrade of roadways by fulfilling one or more geosynthetic functions, including separation, filtration, drainage and stiffening (Zornberg 2017a, 2017b). Base course stabilization involves placing a geosynthetic within or at the bottom of the base course layer to enhance the pavement performance, primarily by providing lateral restraint to the unbound aggregates under traffic loading, ultimately resulting in decreased permanent deformations (e.g. Haliburton *et al.* 1981). The benefits that have been typically sought out in roadway design when incorporating geosynthetics for base course stabilization have been: (1) to reduce the base course thickness required to support traffic loads for a given design life, or (2) to extend the roadway design life, also for the case of traffic loads, for a given base course thickness (e.g. Christopher *et al.* 2006). However, the benefits associated with geosynthetic stabilization of unbound aggregates to mitigate problems associated with environmental loads, while potentially significant, have not been properly documented or quantified.

Several examples of studies conducted to quantify the effectiveness of geosynthetics for base stabilization of flexible pavements with focus on roadway performance under traffic loads include those reported by Al-Qadi *et al.* (1997), Berg *et al.* (2000), Chen *et al.* (2018), Fannin and Sigurdsson (1996), Imjai *et al.* (2019), and Perkins and Ismeik (1997a, 1997b). Roadway performance under traffic loads has been typically quantified by measuring the rutting depth in sections constructed both with and without geosynthetic stabilization (e.g. Al-Qadi *et al.* 2006; Cuelho *et al.* 2014; Tang *et al.* 2014; Sprague and Sprague 2016). However, little if any quantitative study has been conducted to investigate the long-term

performance of geosynthetic-stabilized base courses subjected to environmental loads. Accordingly, the focus of this paper is on quantifying the effectiveness of geosynthetics used in roadways to withstand the environmental loads induced by expansive clay subgrades.

Expansive clays are common in semi-arid regions of Texas, much of central US, and many other regions worldwide. When subjected to moisture fluctuations due to seasonal variations in the precipitation pattern, expansive clays may trigger large volumetric changes that result in ground heave during wet seasons and in settlements during dry seasons. Experience within the Texas Department of Transportation (TxDOT) has shown that these cyclic movements may cause considerable damage to pavement structures, mainly in the form of longitudinal cracks. Roadways constructed over such subgrades have been stabilized using approaches involving lime treatment (Petry and Little 2002) and/or geosynthetics (Zornberg *et al*. 2008a, 2012a, 2012b; Roodi and Zornberg 2012, 2020). In fact, while TxDOT is the US transportation agency with possibly the largest use of geosynthetics in base stabilization projects, the agency has had minimal use of geosynthetics, if any, for conventional base stabilization design objectives (e.g. to reduce the required base thickness due to traffic loads). Instead, geosynthetic-stabilized base courses have been constructed in Texas with the primary objective of mitigating problems associated with expansive clay subgrades. Consequently, systematic quantification and documentation of the long-term field performance of Texas roadways already constructed using geosynthetics to mitigate problems associated with environmental loads present a major data mining opportunity. This is particularly relevant in cases where, judiciously, TxDOT also constructed control test sections with the objective of quantifying in the future the benefits of an innovative design.

This paper presents five case studies of roadways with geosynthetic-stabilized base courses, founded on expansive clay subgrades, and provides a comprehensive analysis of their field performance. This includes the evaluation of full-scale test sections with base courses stabilized using several types of geosynthetics (e.g. biaxial geogrids, multiaxial geogrids, woven geotextiles) as well as of control sections constructed without geosynthetics. The case studies benefit from the availability of long-term field performance data, as multiple seasons are needed to compare the performance of stabilized and control sections in roads constructed over expansive clay subgrades.

2. DISTRESS OF ROADWAYS INDUCED BY THE PRESENCE OF EXPANSIVE CLAY SUBGRADES

Smectite-rich clays, characterized by significant swell-shrink behavior upon changes of moisture content, are common in multiple regions worldwide. In North America, they occur in a large swath including Western Canada, Southern California, Colorado, Nevada, Oklahoma, and Southern and Central Texas (Thornthwaite 1948; Olive *et al*. 1989). O'Neill and Poormoayed (1980) reported that the depth of seasonal variations in soil moisture, for different cities in Texas, ranges from 1.5 to 3 m in Houston (Southern Texas), 2.1 to 4.2 m in Dallas (Northern Texas), and 3 to 9 m in San Antonio (Central Texas).

In areas with arid and semi-arid climates, cycles of wet and dry seasons often result in significant moisture changes in expansive clay subgrades. However, the moisture changes are more substantial near the pavement shoulders, where the subgrade is more prone to precipitation-induced infiltration and evaporation-induced exfiltration than beneath the paved roadway centerline. The non-uniform moisture changes in the expansive clay subgrade lead in turn to non-uniform volumetric changes across the road cross-section. Consequently, as illustrated in Figure 1, differential vertical movements between the edge and centerline of the roadway are expected over recurring wet and dry seasons, when pavement shoulders heave and settle, respectively, in relation to the pavement centerline. Such differential movements induce flexion and, consequently, tensile stresses in the roadway surface layer. Consistent with this mechanism, TxDOT districts have reported the development of longitudinal cracks toward the end of dry seasons (i.e. when tensile strains are greatest) and partial closing of the cracks during wet seasons. Therefore, the presence and extent of these longitudinal cracks, which are known as environmental longitudinal cracks due to the underlying cause for their development, was identified as a suitable indicator to quantify the distress caused by the presence of expansive clay subgrades. Accordingly, the extent of longitudinal cracks in a given road section is quantified herein by the longitudinal crack index (LCI), which corresponds to the ratio between the total length of longitudinal cracks in a road section and the length of the section.

In addition, the crack mitigation ratio (CMR) is defined herein as an index parameter to facilitate

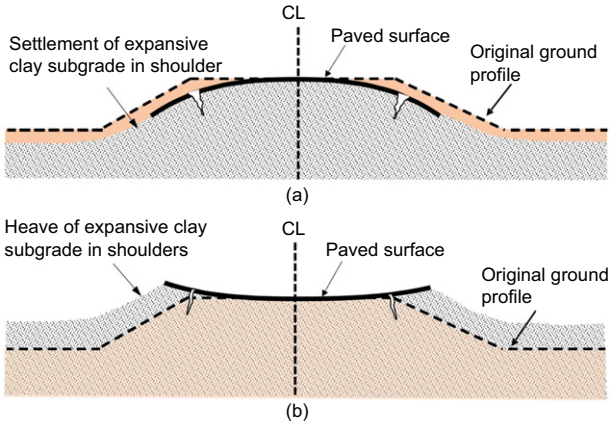

Figure 1. Schematic view of roadway profile on expansive clay subgrades, showing likely locations of environmental longitudinal cracks: (a) dry season; (b) wet season

comparison between the performance of a geosynthetic-stabilized test section and that of its companion control section. The CMR is quantified as the ratio between the LCI in a control section and that in an equivalent geosynthetic-stabilized section (Roodi 2016). This ratio is calculated using control and geosynthetic-stabilized test sections that have been subjected to the same environmental and traffic loads. A CMR value exceeding one indicates that the geosynthetic-stabilized section performed better than the corresponding control section.

3. MITIGATION OF ROADWAY DISTRESS INDUCED BY EXPANSIVE CLAY SUBGRADES

A scheme that has been commonly adopted by TxDOT engineers for roadways over expansive clay subgrades has involved combining geosynthetic stabilization of the base course with lime or cement stabilization of the subbase layer. Specifically, as depicted in Figure 2, materials recycled from the original roadway (including the original surface layer and base course) are mixed, stabilized using lime or cement, and compacted to form the subbase of the new road (Chen 2007). Construction then proceeds by placing the geosynthetic over the stabilized subbase, then the new base course and finally an asphaltic surface layer. The shoulders of the rehabilitated road are often extended to provide additional lateral support.

While several roadways have been repaired using the aforementioned scheme involving geosynthetics, the performance of the repaired roadways had not been previously quantified nor systematically evaluated. Consequently, the projects identified as part of the investigation documented in this paper include the case studies that involve geosynthetic-stabilized sections and that are also founded on clay subgrades (ranging from comparatively low to high expansiveness). Long-term performance of the case studies was quantified with focus on the potential benefits of using geosynthetics for distress mitigation.

The main characteristics of the five case studies evaluated in this paper are summarized in Table 1. Eight types of geosynthetics (referred to as GS1 through GS8), involving a wide range of physical and mechanical properties as well as manufacturing processes, were used in the test sections constructed as part of those projects. Specifically, the geosynthetics involved in this study included two integrally-formed polypropylene (PP) biaxial geogrids, three integrally-formed PP multiaxial geogrids, a woven PP geotextile, a laser-bonded PP biaxial geogrid, and a polyester (PET) biaxial geogrid. Table 2 summarizes the main characteristics of the various geosynthetics used in the five case studies (as reported by the geosynthetic manufacturers). They were all selected by TxDOT following the specifications in use at the time of roadway construction.

Climatic and environmental characteristics of the locations of the five case studies were also evaluated. As illustrated in Figure 3, the five case studies are located in a region that is characterized by a Subtropical Humid climate (Larkin and Bomar 1983). This climate zone is characterized by comparatively short, cold, and wet winters along with warm and long summers. The relative

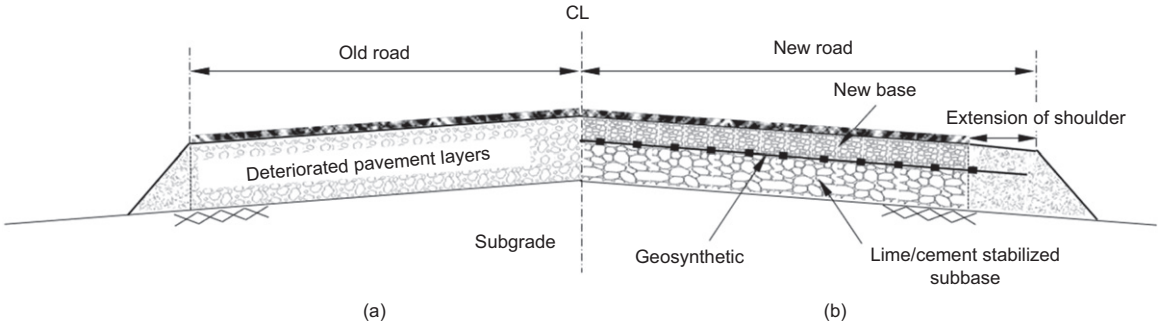

Figure 2. Typical repair scheme for TxDOT roadways founded on expansive clay subgrades: (a) before retrofitting; (b) after retrofitting using geosynthetic-stabilization of the base layer

Table 1. Characteristics of the roadways with geosynthetic-stabilized base course evaluated as field case studies in this paper

Case Study[a]	Texas county	Construction year	ADT at time of construction	Number of test sections	Geosynthetic(s)[b]	Geosynthetic location
Case Study A	Milam	1996	180	3	GS1	Base-subbase interface
Case Study B	Grimes	2002	1100	2	GS1, GS2	Base-subbase interface
Case Study C	Travis	2001 and 2007	7400	3	GS1	Base-subbase interface
Case Study D	Lee	2011	5300	5	GS1, GS3, GS4, GS5, GS6	Base-subbase interface
Case Study E	Grimes	2006	880	32	GS1, GS7, GS8	Base-subbase interface

ADT, average daily traffic.
[a]Case Study A: FM1915; Case Study B: FM1774; Case Study C: FM734; Case Study D: SH21; Case Study E: FM2.
[b]Geosynthetic characteristics are presented in Table 2.

Table 2. Characteristics of the geosynthetics used in the test sections of the different field case studies

Geosynthetics	Geosynthetic type	Polymer	Manufacturing process	Aperture size (mm)	Percent open area (%)	Thickness (mm)			In-isolation tensile modulus (J) @2% elongation, (kN/m)		In-isolation ultimate tensile strength, (kN/m)	
						MD Ribs	CMD Ribs	Junctions	MD	CMD	MD	CMD
GS1	BXGG	PP	Extruded	25 × 33	75	0.76	0.76	1.5	205	330	12.4	19
GS2	BXGG	PP	Laser bonded	44 × 44	75	0.77	0.77	1.5	300	500	20	32
GS3	BXGG	PP	Extruded	33 × 33	70	0.76	0.76	n/a	200	275	8	10.5
GS4	MXGG	PP	Extruded	33 × 33 × 33	>70	1.5[a]	1.2[b]	3.1	200[c]	200[c]	No data	No data
GS5	MXGG	PP	Extruded	40 × 40 × 40	>70	1.3[a]	1.2[b]	3.4	No data	No data	No data	No data
GS6	MXGG	PP	Extruded	40 × 40 × 40	>70	2.0[a]	1.6[b]	3.8	No data	No data	No data	No data
GS7	BXGG	PET	Woven junctions	25 × 25	>70	No data	No data	No data	365	365	29.2	29.2
GS8	WGT	PP	Woven	n/a	n/a	n/a	n/a	n/a	700	965	70	70

BXGG, biaxial geogrid; MXGG, multiaxial geogrid; WGT, woven geotextile; PP, polypropylene; PET, polyester; MD, machine direction; CMD, cross machine direction; n/a, not applicable.
[a]In diagonal direction.
[b]In transverse direction.
[c]Radial stiffness @ 0.5% strain.

humidity is typically high, and the temperature is rarely below freezing point. Figure 3 also shows the contour lines for Thornthwaite Moisture Index (TMI), as specified by Thornthwaite (1948), around the locations of the case studies. This index has been defined by Thornthwaite based on the 'humidity' and 'aridity' indexes and the 'water need' in the region. As presented in Figure 3, all case studies were located between contour lines of TMI = −20 and TMI = + 20, which are characterized as 'dry subhumid (C1)' to 'moist subhumid (C2)' climatic types by Thornthwaite (1948).

Environmental data were collected from the weather stations located in the vicinity of the case studies from the National Centers for Environmental Information's (NCEI's) latest three-decade averages of climatological variables, also known as the National Oceanic and Atmospheric Administration's (NOAA's) US 1981–2010 Climate Normals (Arguez *et al*. 2010). The three-decade mean for the minimum and maximum daily temperature had a narrow range among the various weather stations. The three-decade mean for minimum daily temperature ranged from 12.8 to 14.9°C and for the maximum daily temperature ranged from 25.8 to 26.3°C. The mean annual average temperature was also found to have a narrow range among various weather stations ranging from 19.2 to 20.5°C (Figure 4). The mean annual precipitations during the same period ranged from approximately 875 mm to 1150 mm for various weather stations.

Additional environmental data were collected from three weather stations located in the vicinity of the five case studies. Approximate locations of the three weather stations and of the five case studies are shown in Figure 3. Weather Station 1 is located comparatively close to Case Study A, Weather Station 2 is near Case Studies B and E and Weather Station 3 is in the vicinity of Case Studies C and D.

The mean daily temperature and relative humidity values gathered from the three weather stations over a 9-year period (from 2006 to 2015) are presented in Figure 4. This figure also shows the mean annual average temperature from the NOAA's 1981–2010 Climate Normals. The three weather stations recorded consistent cyclic temperature variations ranging from low mean daily temperatures of 7 to 10°C in December and January to high mean daily temperatures of 27 to 32°C in mid-summer. However, the low temperatures recorded at Weather Station 2 were slightly higher than those in Weather Stations 1 and 3.

The changes in mean daily humidity, presented in Figure 4, also show similar trends among the three weather stations. High-humidity periods lasting over several months have been intermittently followed by few, comparatively low-humidity months. Overall, Weather Station 2 recorded comparatively higher humidity values than Weather Stations 1 and 3. The highest humidity values in Weather Station 2 ranged from 85 to 90% while the lowest humidity value from this weather station was recorded in 2011 and corresponds to approximately 60%. On the other hand, the lowest humidity recorded in 2011

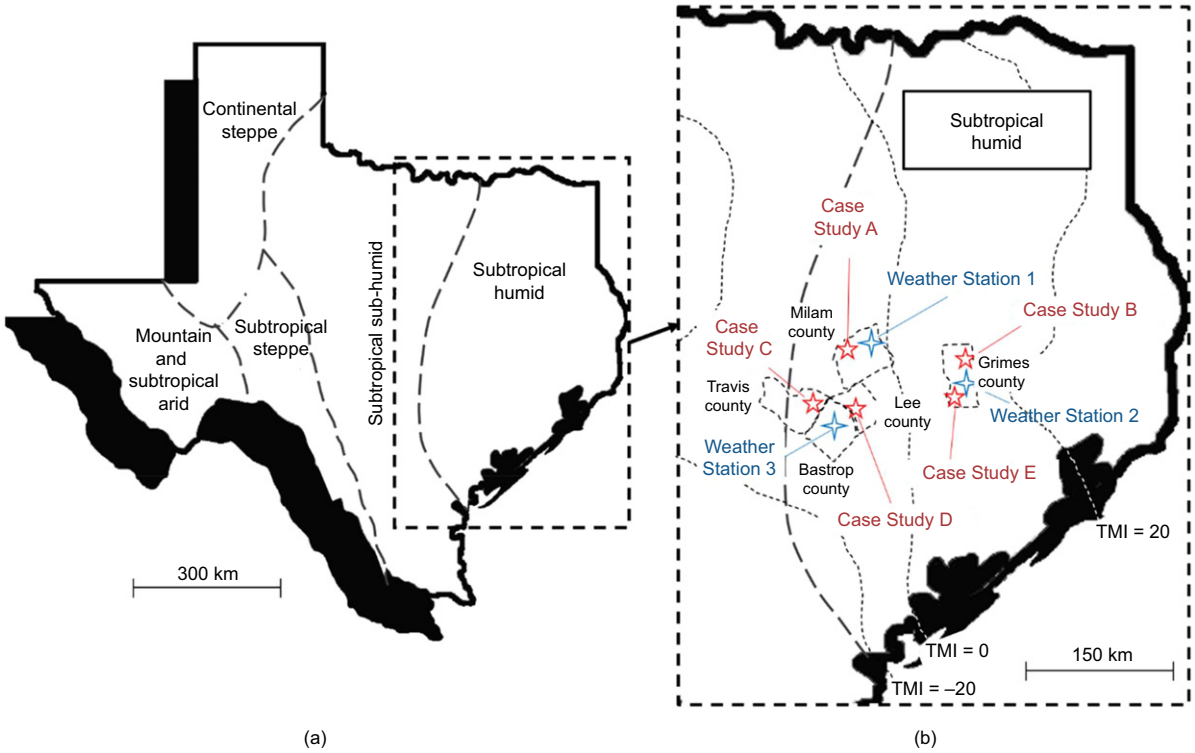

Figure 3. Climatic regions in Texas (adapted after Larkin and Bomar 1983) along with Thornthwaite Moisture Index (TMI) contours (Thornthwaite 1948): (a) climate regions map; (b) detail showing locations of case studies and weather stations and the TMI contours

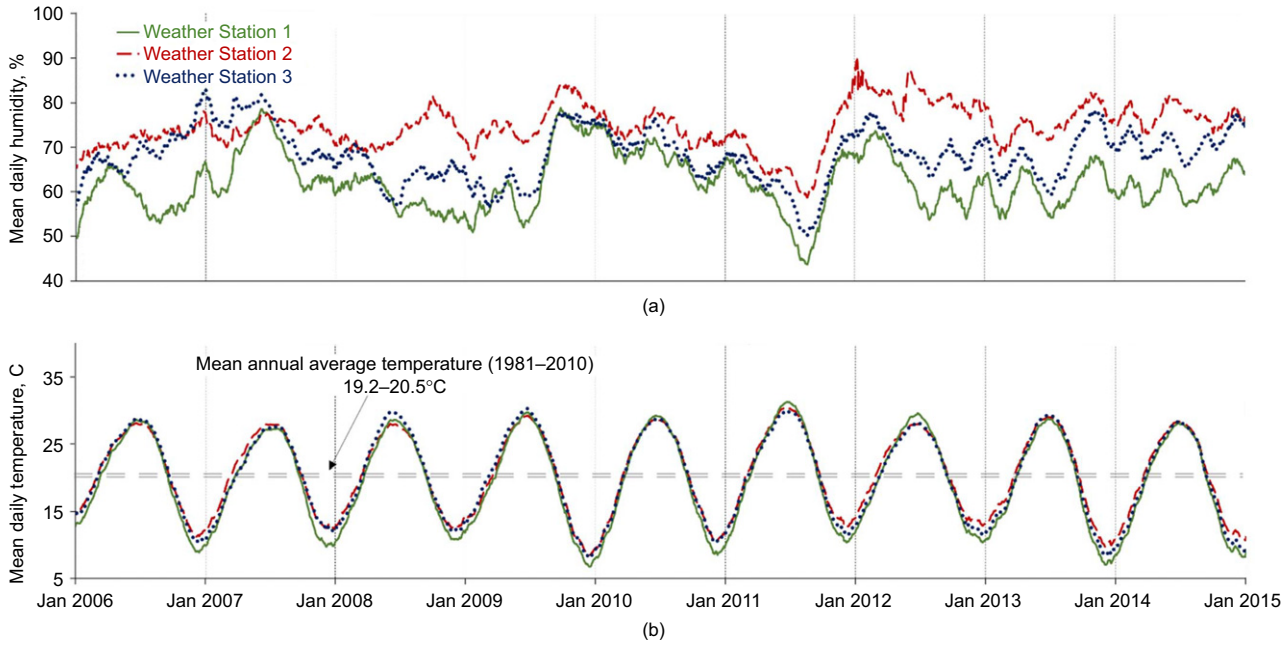

Figure 4. Mean daily climatic data at three weather stations (2006 to 2015): (a) humidity; (b) temperature

from Weather Stations 1 and 3 was 50 and 44%, respectively. The highest humidity values recorded in Weather Stations 1 and 3 were 79 and 82%, respectively.

The comparatively higher humidity (and slightly higher low temperature values) recorded at Weather Station 2 can be attributed to its location toward the east of Weather Stations 1 and 3. A general trend in the eastern Texas climate involves gradual reduction in precipitation along with gradual increase in the high temperature value (and decrease in the low temperature value) toward the West. Precipitation data at the three weather stations presented in Figure 5 is consistent with the humidity trends. This figure shows cumulative annual precipitation at the three weather stations for the same 9-year period evaluated for temperature and humidity. Overall, Weather Stations 1 and 3 (Figures 5a and 5c) recorded a lower rainfall than

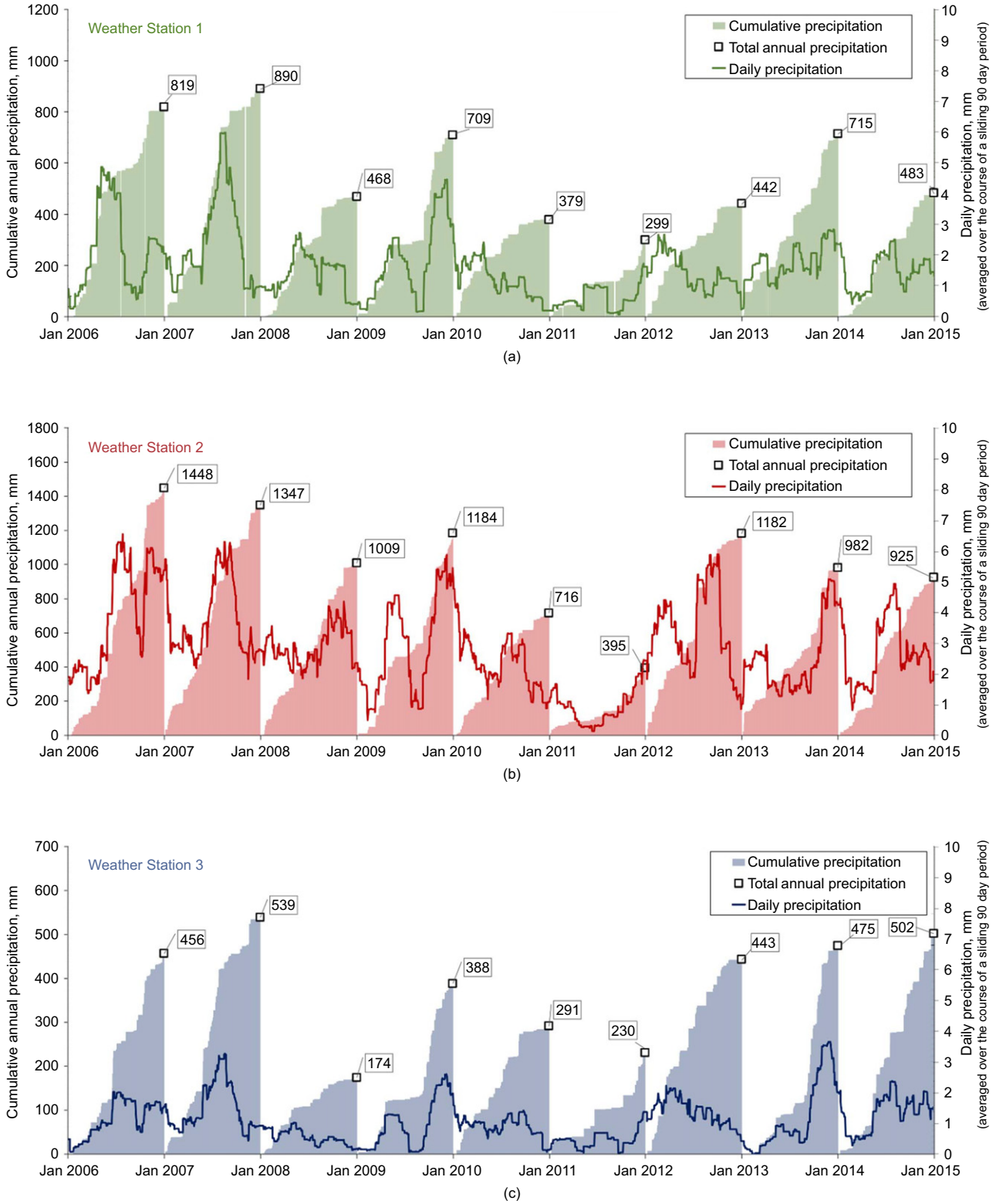

Figure 5. Cumulative annual and daily precipitation (2006–2015): (a) Weather Station 1; (b) Weather Station 2; (c) Weather Station 3

Weather Station 2 (Figure 5b). However, several cycles of wet and dry years can be identified in all three weather station data sets. Specifically, the years 2010 and 2011 have been among the driest years for all three weather stations and the years 2006, 2007, and 2013 have been among the wettest years for all three weather stations. Figure 5 also shows the daily rainfall averaged over the course of a sliding 90-day period centered on each day. Evaluation of the changes in daily rainfalls (solid lines in Figures 5a–5c) over time indicates that the data sets from all three weather stations show numerous intermittent dry and wet seasons.

Evaluation of the climatic characteristics from the three weather stations indicates that, overall, all case studies have been exposed to multiple wet and dry cycles over the time during which their performance was evaluated in this

study. Although specific weather conditions may have been different among the different case studies, various test sections in each case study have been subjected to the same environmental conditions.

The design of the drainage systems was similar among the various case studies evaluated in this paper. Specifically, all the roadway sections were uncurbed and centerline-crowned with roadway surfaces being out-sloped at a typical inclination of 2% toward each side of the road. The crowned profile of the roadway allowed the discharge of rainwater from the roadway surface onto the shoulders and eventually into conventional v-shaped ditches on both roadsides. Inspection of the test section surfaces during site visits conducted in different seasons did not show water ponding or distress associated with water ponding on the roadway surface, indicating adequate pavement drainage systems.

Vegetation conditions of the lands corresponding to the roadways considered in this paper were also assessed. Overall, the ground surface in the different case studies involved grasslands where regional grasses and forbs were the dominant types of vegetation. While tracking of mowing and of vegetation changes was not possible at each site, observations during site visits indicated that mowing of grasses on both sides of the roadways was conducted regularly. Although frequency of mowing and vegetation types may have differed among the various case studies, it should be noted that the vegetation conditions were observed to be essentially the same among the various test sections in each of the case studies.

3.1. Case Study A: FM1915

3.1.1. *Site description*

Farm-to-Market (FM) road 1915 is located in Milam County, Texas. Significant longitudinal cracks had been reported along a 4 km portion of road, extending west of the Little River Relief Bridge, due to the presence of high plasticity clays in the subgrade. As part of a 1996 rehabilitation plan, the original pavement was removed in its entirety and was recycled to build a 250 mm-thick subbase stabilized with 5% lime. As shown in Figure 6, three test sections were constructed using different design schemes. Section A2 was a control section (i.e. without geosynthetics) with a 180 mm-thick base layer, whereas a biaxial geogrid (GS1) was placed at the interface between the subgrade and the base layer in Sections A1 and A3. While Section A3 was constructed with the same base thickness as that of the control section, Section A1 was constructed with a thinner base layer (130 mm) with the objective of also evaluating the potential reduction of base thickness requirements when adopting geosynthetic stabilization.

The characteristics of geosynthetic GS1, the biaxial geogrid placed in Case Study A at the base-subbase interface, are listed in Table 2. Table 3 summarizes the results of a soil investigation conducted to characterize the base and subgrade soils at the locations of the FM1915 test sections (Dessouky *et al.* 2012). Base and subgrade soil samples were collected from the various sections using mechanical augers. The subgrade Plasticity Index (PI) was found to range from 30 to 56, indicating the presence of highly plastic subgrade soils in all test sections.

Shrinkage test results, presented in Table 3, indicate that the linear shrinkage measured for the subgrade samples ranged from 15% to 31%. Sulfate concentration tests, conducted using a colorimeter according to test procedures in Tex-145-E, indicated that the sulfate content in all test sections was negligible.

The unbound aggregates in the base layer were characterized by an optimum moisture content of 7.4% and a maximum dry unit weight of 17.9 kN/m^3 according to the standard Proctor test (600 kN-m/m^3 compaction energy), obtained following ASTM D698.

3.1.2. *Site performance evaluation*

Two series of falling weight deflectometer (FWD) tests were conducted on the FM1915 test sections, with the first series conducted in July 2001 (Zornberg *et al.* 2008b).

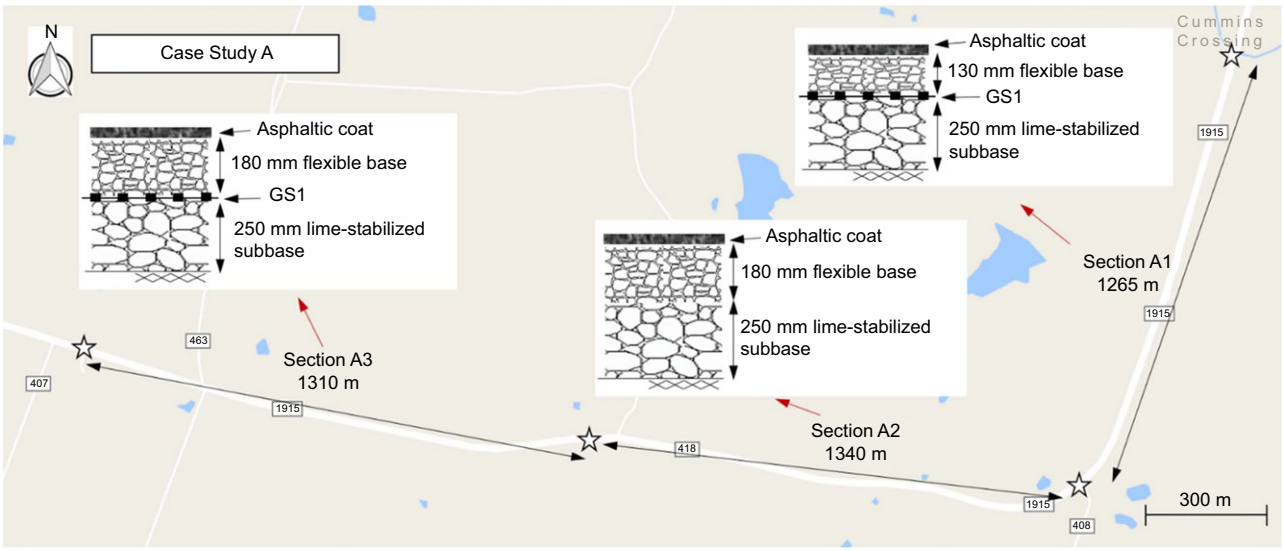

Figure 6. Layout of FM1915 test sections and corresponding road profiles (Case Study A)

Table 3. Characteristics of subgrade soils in the different field case studies

Test/procedure	Parameter	Case Study A[a]			Case Study B		Case Study C[a]		Case Study D[b]	Case study E
		Sec.1	Sec.2	Sec.3	Sec.1	Sec.2	Sec.1	Sec.2		
Sieve analysis	Fines content, %	63	77	47	>50	>50	67	64	65	60
Standard Proctor compaction	Optimum water content, %	26	28	18	No data	No data	No data	No data	20	32
	Maximum dry unit weight, γ_d, kN/m^3	13.5	13.7	17.1	No data	No data	No data	No data	15.4	15.5
Atterberg limits	Liquid limit (LL)	83	73	49	57–65	43–48	No data	No data	40–58	72
	Plastic limit (PL)	27	34	19	20–22	14–16	No data	No data	17–20	33
	Plasticity index (PI)	56	39	30	37–43	28–33	>35 (PI = 9 for lime- treated specimens)	>35 (PI = 9 for lime-treated specimens)	26–41	39
Soil classifications	USCS classification	CH	CH	SC	CH	CL	CH	CH	CH	CH
Shrinkage	Linear shrinkage, %	31	25	15	No data	No data	2 (for lime-treated specimens)	3 (for lime-treated specimens)	No data	No data
Sulfate concentration	Sulfate content, ppm	~ 0	~0	~0	No data	No data	<100	190	1290	~0
Potential vertical rise	PVR, mm	No data	No data	No data	30–65	30–45	No data	No data	No data	78

[a]From Dessouky *et al.* (2012).
[b]From Armstrong (2014).

Beginning in Section A1, tests were conducted at 30.5 m intervals along the entire 4 km of the project. Deflection data obtained from the FWD tests was analyzed using the MODULUS 6.0 software (Scullion 2004) to obtain the average layer moduli for each pavement section layer through back calculation. As summarized in Table 4, the resilient modulus back calculated using FWD test data indicates that the modulus in Section A1 was slightly higher than those in Sections A2 and A3. The moduli values obtained from the second FWD test series, conducted in 2012, are also summarized in Table 4 (Dessouky *et al.* 2012). Evaluation of these results shows smaller decrease with time of moduli values in the geosynthetic-stabilized sections (i.e. Sections A1 and A3) than in the control section (i.e. Section A2). Specifically, comparison of the moduli predicted from the two FWD test series indicates that the base course moduli decreased by 24% (from 1725 to 1310) in Section A1 and by 6% (from 1450 to 1360) in Section A3. On the other hand, the base course modulus decreased by 39% (from 1655 to 1015) in Section A2. These performance data underscore the comparatively faster degradation of the base course modulus in the control section than in the geosynthetic-stabilized sections.

Evaluation of the pavement layer moduli obtained from correlations with dynamic cone penetrometer (DCP) test results, conducted in 2012, also demonstrates the beneficial effect of using geosynthetics in Sections A1 and A3. Specifically, use of these correlations resulted in base course moduli of 980 and 655 MPa for geosynthetic-stabilized Sections A1 and A3, respectively, whereas a modulus of 285 MPa was obtained for control Section A2 (Table 4). Considering that base moduli are expected to have been the same (or similar) in the three test sections at the time of construction, the DCP test results also indicate that degradation of the roadway structural layers was reduced when adopting the use of geosynthetics for base stabilization.

The performance of FM1915 was also evaluated using performance data collected using TxDOT's Pavement Management Information System (PMIS) database. Specifically, changes in LCI were evaluated for each test section from 1998 to 2014. As summarized in Figure 7, LCI results indicate that the two geosynthetic-stabilized sections (A3 and A1) performed significantly better than the control section (A2). The average LCI obtained in 2014 for Section A3 (geosynthetic-stabilized section with base thickness equal to that of the control section) was found to be particularly small (approximately 16%). Instead, the average LCI in Section A1 (geosynthetic-stabilized section with reduced base thickness) was approximately 26%, while the average LCI in Section A2 (control section) was approximately 33%. These results indicate that use of the geosynthetic adopted in this project for base stabilization resulted in a performance equivalent to using a thickness of at least 50 mm additional base course (i.e. it was equivalent to a reduction of approximately 28% of the original 180 mm-thick base layer). The corresponding CMR values for Sections A1 and A3 are 2.1 and 1.3,

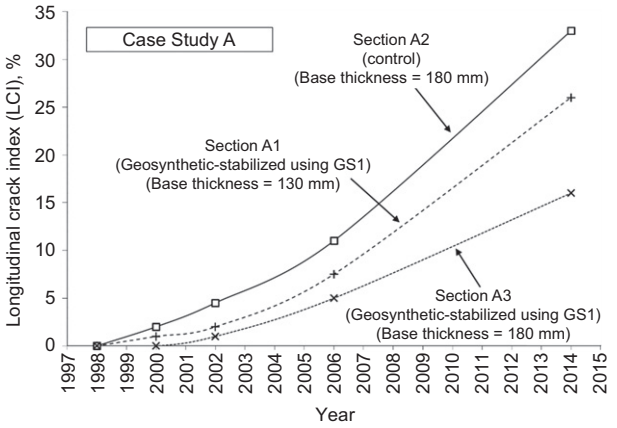

Figure 7. Longitudinal crack index (LCI) from 1998 to 2014 at the FM1915 test sections (Case Study A)

respectively, further underscoring the reduction in longitudinal cracking when adopting a geosynthetic-stabilized base. Figure 8 shows the FM1915 road conditions from a 2017 condition survey, illustrating that clearly more significant longitudinal cracks have developed in the control than in the geosynthetic-stabilized sections.

3.2. Case Study B: FM1774

3.2.1. *Site description*

Over 14 km of FM1774, extending from SH90 to FM2445, were reconstructed in August 2002 as part of the restoration of distressed roads in Grimes County, Texas. Evaluation of the original pavement structure

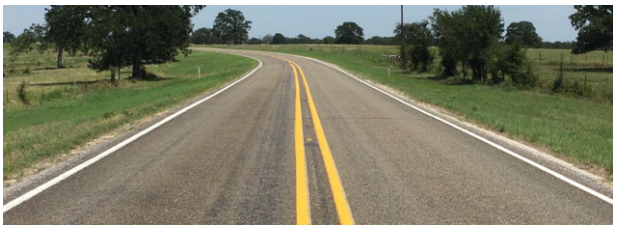

(a)

(b)

Figure 8. Roadway conditions at the FM1915 (Case Study A) test sections in 2017: (a) Section A1 (geosynthetic-stabilized section); (b) Section A2 (control section)

Table 4. Average layer moduli for various layers of roadways in Case Studies A and C, obtained through back calculation of field measurements

	M_r in Case Study A (MPa)								M_r in Case Study C (MPa)			
	Sec.1 (GS-stabilized)			Sec.2 (Control)			Sec.3 (GS-stabilized, reduced base thickness)			Sec.1 (Control)		Sec. 2 (GS-stabilized)	
	From FWD[a] (2001)	From FWD[b] (2012)	From DCP[b] (2012)	From FWD[a] (2001)	From FWD[b] (2012)	From DCP[b] (2012)	From FWD[a] (2001)	From FWD[b] (2012)	From DCP[b] (2012)	From FWD[b] (2012)	From DCP[b] (2012)	From FWD[b] (2012)	From DCP[b] (2012)
Surface layer	2070	1375	No data	2060	1375	No data	2020	1375	No data	2885	No data	2250	No data
Base course	1725	1310	980	1655	1015	285	1450	1360	655	760	490	1000	555
Subbase course	440	615	490	380	390	230	305	880	490	760	490	1000	555
Subgrade	138	90	83	130	75	62	130	117	193	105	92	130	115

[a]From Zornberg *et al.* (2008a, 2008b).
[b]From Dessouky *et al.* (2012).

revealed the presence of up to 215 mm of seal coats and asphaltic concrete, 75 to 350 mm of flexible base, and a brown, gray and tan sandy clay subgrade in most areas. However, additional investigations of the subgrade soils also indicated the presence of more expansive clays under two portions of the roadway (0.5 and 3.4 km-long road portions). The original road was fully removed, and the excavated material was recycled to construct a 250 mm-thick lime-stabilized subbase. Construction also included a new 175 mm-thick base course and a thin asphaltic course layer. In addition, a geogrid layer was installed at the subbase-base interface in the two portions of the roadway where the presence of expansive clay subgrade soils had been identified. However, to evaluate the suitability of the geogrid specifications available at the time, each portion was considered an experimental test section, and was constructed using two different geogrid materials that met the TxDOT specifications available at the time. Accordingly, Test Section B1 (approximately 500 m long) was constructed using an integrally formed polypropylene geogrid (GS1) while test Section B2 (approximately 3400 m long) was constructed using a laser-bonded polypropylene geogrid (GS2). Figure 9 illustrates the layout and section profiles of these two FM1774 test sections, which differed primarily on the geosynthetic selected in each case for stabilization.

As part of the subgrade soil investigation conducted before reconstruction, a total of 13 borings were drilled along the project limits to depths of approximately 3 m. As summarized in Table 3, characterization of soil samples collected from the borings located within the limits of the test sections indicated the presence of a highly expansive clay under test Section B1 (average PI of approximately 35) and a medium to highly expansive clay under test Section B2 (average PI of approximately 30). The potential vertical rise (PVR), which is the potential heave in a soil profile if moisture in the different soil layers increases from an initial reasonably dry to a saturated condition (TxDOT 2014), was estimated at the boring locations along FM1774. An active moisture fluctuation zone of 2.1 m was considered in these evaluations. The PVR was predicted to range from 30 to 65 mm for the borings located in Section B1 and from 30 to 45 mm for the borings located in Section B2. Use of geosynthetic to stabilize the two portions of the road was then adopted since design criteria required that the PVR should not exceed 40 mm.

3.2.2. *Site performance evaluation*

Results from condition surveys conducted in the summer of 2004 indicated clear differences between the performances of Sections B1 and B2. While Section B1, stabilized with GS1, had a relatively small number of longitudinal cracks (Figure 10), a significant number of longitudinal cracks was observed in Section B2, stabilized with GS2. One of the longitudinal cracks that developed in Section B2 is presented in Figure 11, which shows the road conditions before and after a forensic excavation. It was determined that the junctions of geogrid GS2 had often failed. The junction breakage led to slippage of the transverse geogrid members at this location (Figure 11b).

An evaluation of the performance data from TxDOT's PMIS database for 2017 was also conducted to assess comparatively recent conditions of the FM1774 test sections. Specifically, the performance of the test sections was evaluated using ride quality data, LCI, and condition scores. The ride quality is often characterized using the International Roughness Index (IRI), which is an open-ended range index (expressed in meters per kilometer). High IRI values correspond to high longitudinal road roughness and, consequently, to less favorable ride quality. Also, comparatively more significant increases in IRI correspond to more severe degradation of road condition. As presented in Figure 12a, both left and right wheel paths in Section B1 showed lower changes in IRI than the left and right wheel paths in Section B2. The average PMIS condition scores of the FM1774 test sections are presented in Figure 12b. The PMIS condition score

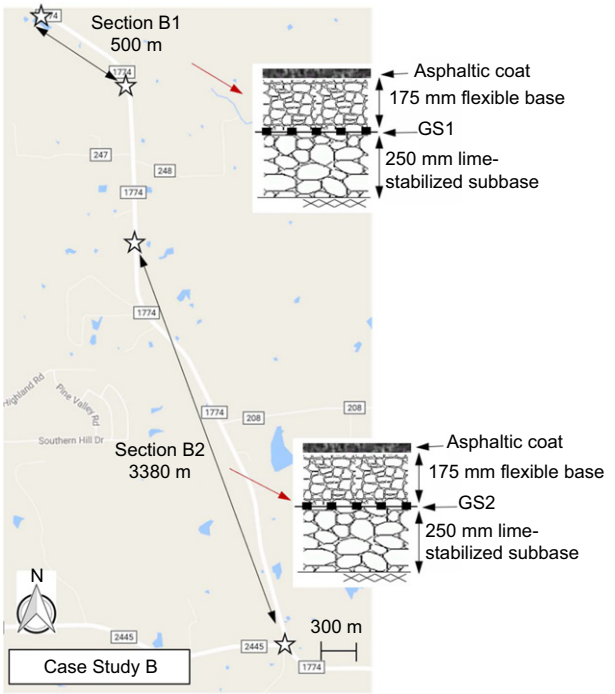

Figure 9. Layout of FM1774 test sections and corresponding road profiles (Case Study B)

Figure 10. View of road conditions in 2004 at the FM1774 test section stabilized using GS1 in Case Study B

Figure 11. View of longitudinal cracks observed in 2004 at FM1774 test section stabilized using GS2 in Case Study B: (a) view of longitudinal crack on pavement surface; (b) view during forensic evaluation exposing geogrids showing junction failure at location of longitudinal crack

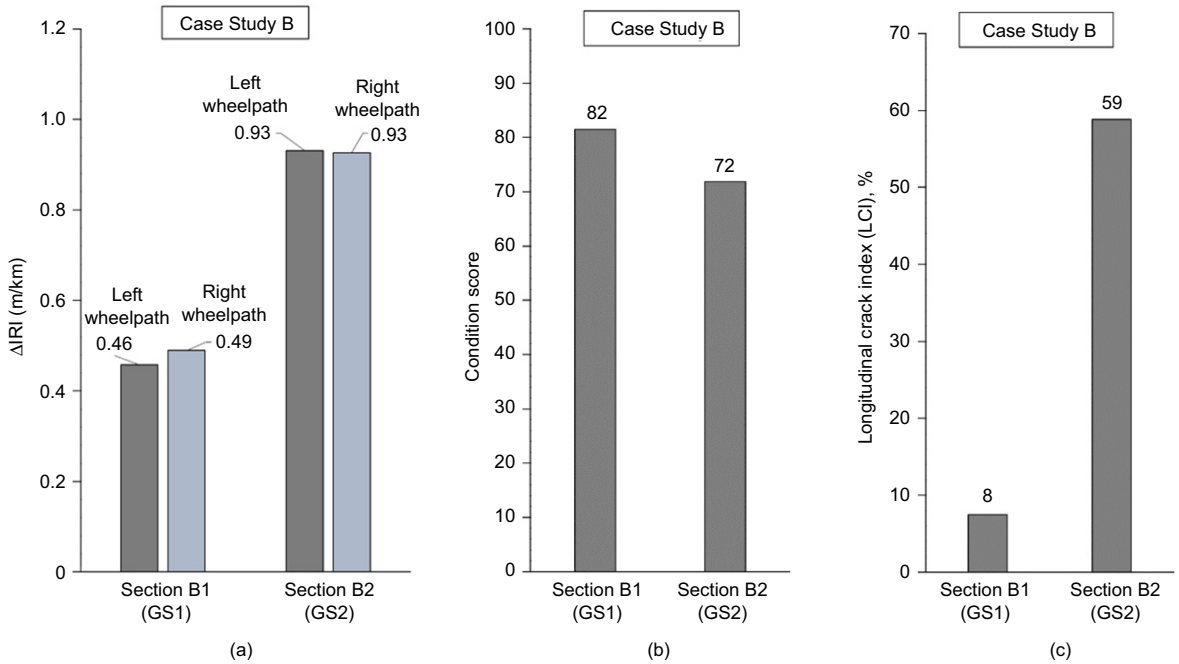

Figure 12. Comparative performance of FM1774 test sections (Case Study B) based on 2017 TxDOT PMIS data: (a) change in IRI; (b) condition score; (c) LCI

combines ride quality measurements and pavement distress ratings into a single description of overall pavement condition. The condition score, adjusted for traffic and speed, is expressed using values ranging from 1 (worst condition) to 100 (best condition) and classes ranging from 'very poor' to 'very good.' As shown in Figure 12b, on average, Section B1 had a better condition score than Section B2 (82 for Section B1, 72 for Section B2). Based on these 2017 condition scores, several portions of test Section B2 were rated as 'fair' and 'poor' conditions. On the other hand, Section B1 received 'good' condition ratings.

Finally, as presented in Figure 12c, the LCI in Section B1 was significantly lower than that in Section B2. While

the average LCI in Section B1 was below 10%, it reached almost 60% in Section B2. Results from a subsequent condition survey, conducted at FM1774 in 2017, also highlighted important differences between the extent of longitudinal cracks in Sections B1 and B2. Severe cracking at the edge and in the paved area of Section B2 could be observed during the 2017 condition survey (Figure 13a). Breaks in laser-bonded junctions between GS2 longitudinal and transverse ribs were identified in areas where geosynthetics were exposed (Figure 13b). On the other hand, Section B1 showed a very good overall condition (Figure 13c).

The significant difference in performance between test sections stabilized using GS1 and GS2 led to a reevaluation of the TxDOT geogrid specifications available at the time. This is because the geogrid specifications available at the time of construction (TxDOT DMS-6270 (TxDOT 2010)), met by both GS1 and GS2, required an ultimate tensile strength exceeding 12.4 kN/m, tensile modulus at 2% strain exceeding 197.3 kN/m, junction strength exceeding 89.1 N, and percent open area exceeding 60%. In fact, the poorly performing geogrid GS2 had ultimate strength and tensile modulus exceeding those of GS1 (Table 2). Evaluation of the field performance indicates that the specifications for geogrid selection used at that time for base stabilization applications did not necessarily lead to adequate field performance. It should be noted that the properties defined by the specifications available at that time involved only geosynthetic properties obtained in isolation (i.e. without the confinement of soil) or at ultimate condition state (e.g. tensile strength), which may have not adequately accounted for the actual performance of geosynthetic-stabilized base layers. Specifically, while the two biaxial geogrids used at this site had adequate in-isolation properties, they led to significantly different levels of improvement. Revised geogrid specifications, adopted by TxDOT after construction of FM1774, include in-soil mechanical properties of geosynthetics. Subsequent evaluations using the subsequently revised TxDOT specifications, which include in-soil mechanical property requirements, show that the differences in performance could have been captured with the new specifications (Roodi *et al.* 2018).

(a)

(b)

(c)

Figure 13. Images collected during 2017 condition survey at FM1774 (Case Study B): (a) extensive cracks observed in Section B2; (b) view of junction failure in GS2 used in Section B2; (c) view of comparatively good condition (no cracks) in Section B1

3.3. Case Study C: FM734

3.3.1. *Site description*

FM734, located in Austin, TX, underwent reconstruction in 2001 along a 4.8 km portion of the roadway from Samsung Rd. to State Highway (SH) 130. This portion presented severe distress in the form of longitudinal cracks, as well as frequent swells and dips. The distress was initially attributed to sulfate heave as well as to seasonal swelling and shrinkage of the underlying expansive clay subgrade. As shown in Figure 14, the longitudinal cracks on the road were significant, with crack width sometimes exceeding 25 mm. The pavement profile in the portion of FM734 evaluated in this paper involved a 250 mm-thick hot mix asphalt (HMA) layer, underlain by a 305 mm-thick base course and a 200 mm-thick lime-stabilized subgrade (Figure 15).

FM734 was reconstructed in two stages, completed in 2001 and 2007. Reconstruction plans were constrained by

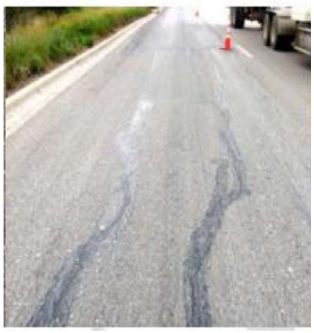

(a)

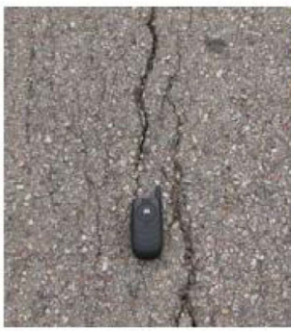

(b)

Figure 14. Conditions at FM734 (Case Study C) before rehabilitation (photo courtesy of TxDOT): (a) longitudinal cracks on the road; (b) close-up view of longitudinal cracks

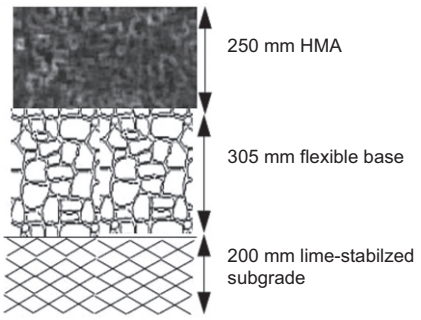

Figure 15. FM734 profile before rehabilitation (Case Study C)

limited right-of-way, traffic control considerations and the need to utilize locally available materials. To address concerns regarding the detrimental use of lime stabilization in potentially sulfate-rich subgrade soils, reconstruction involved removing the entire pavement structure and partial excavation into the subgrade layer. Materials from the old pavement (i.e. HMA and base course) were recycled and used in the new road.

In 2001, two test sections (Sections C1 and C2) were constructed from Harris Branch Parkway to SH130 to evaluate various approaches proposed to mitigate problems associated with the expansive clay subgrade. The layout and designs of the FM734 test sections are presented in Figure 16. The same profiles, involving a 250 mm-thick new base course overlain by a 200 mm-thick HMA layer, were used in both sections. However, while Section C1 was constructed on a 200 mm-thick lime-stabilized subgrade, Section C2 was stabilized with a biaxial geogrid (GS1) placed at the interface between the natural subgrade and the new base layer. The performance of test Sections C1 and C2 was evaluated from 2001 to 2006. Findings from the performance evaluation of Sections C1 and C2 were then adopted for the final design considered in the 2007 reconstruction of the main portion of the road (Section C3). As subsequently explained, the comparatively better performance of Section C2 led to adopting the use of geosynthetic stabilization in Section C3, which extended from Samsung Blvd. to Harris Branch Parkway. Section C3 was constructed using a geogrid (GS1) placed between a 100 mm-thick subbase layer and a 460 mm-thick base layer. The subbase consisted of recycled asphalt pavement (RAP), while the base course involved a 50/50 mixture of salvaged base and RAP, stabilized with 3% cement. The use of recycled materials for construction of the base course, adopted because of environmental and cost considerations, led to the increased thickness of the base course compared to those in Sections C1 and C2. Section C3 was paved using a 200 mm-thick HMA.

Preliminary evaluation of the natural subgrade in the test sections indicated high plasticity clays (PI values exceeding 35). Results from tests conducted on lime-stabilized samples collected from the expansive clay subgrade in Sections C1 and C2 are presented in Table 3 (Dessouky *et al.* 2012). Characterization test results for lime-treated soil samples indicate relatively low shrinkage and PI values. Specifically, lime treatment was found to decrease the PI of the treated subgrade to values as low as 9 and the linear shrinkage to values under 5%. The sulfate content was below 200 ppm. Overall, the data in Table 3 indicates that subgrade soil properties in Section C1 were similar to those in Section C2.

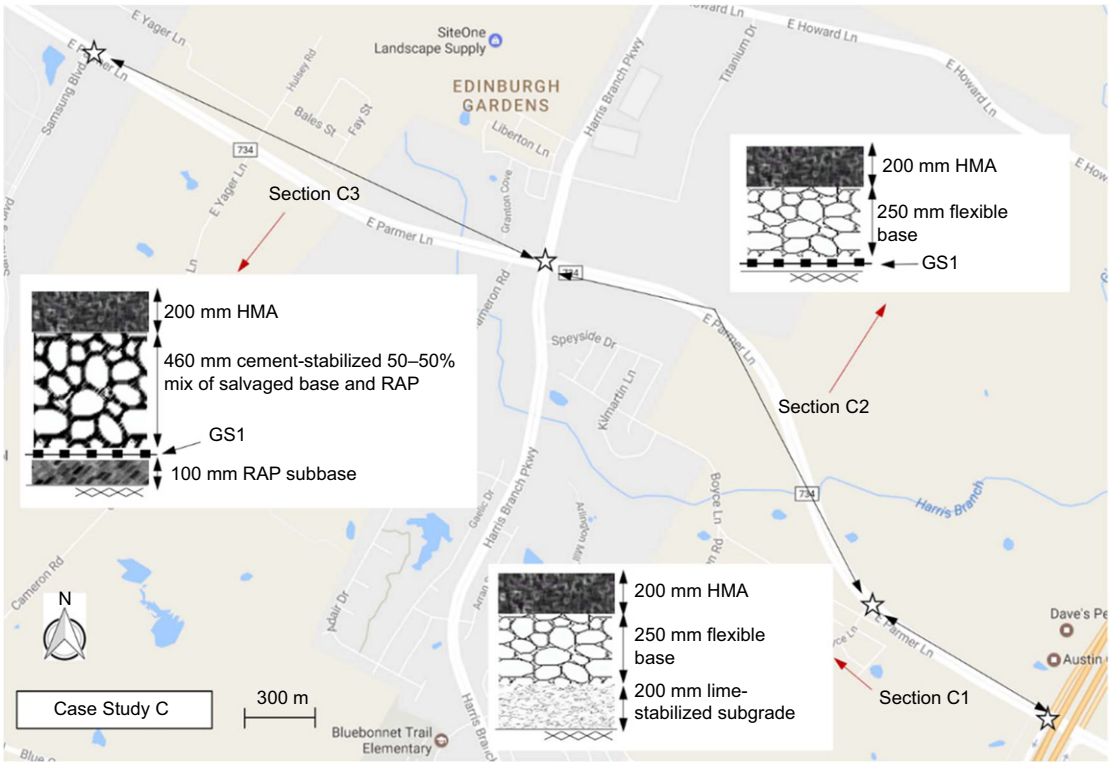

Figure 16. Layout of FM734 test sections and associated road profiles (Case Study C)

The unbound aggregate in the base layer in Sections C1 and C2 was characterized by an optimum moisture content of 8 to 9% and maximum dry unit weight of 20.6 to 21.2 kN/m^3 according to the standard Proctor test following ASTM D698. The characteristics of GS1, the geosynthetic layer used at the base-subbase interface, are summarized in Table 2.

3.3.2. *Site performance evaluation*

The performance of Sections C1 and C2 was evaluated from 2001 to 2006 by comparing ride quality data (using IRI) and visual assessment of road conditions. Specifically, the change in IRI for Sections C1 and C2 was evaluated from 2004 to 2007. Section C1 (control) was found to have an average change in IRI of approximately 0.50 m/km and to present severe dips, heaves and longitudinal cracks. Instead, Section C2 (stabilized using GS1) was characterized by an average change in IRI of approximately 0.15 m/km, having a significantly lower number of longitudinal cracks, dips and bumps. Therefore, geosynthetic stabilization was determined to be a more appropriate technique than lime stabilization to mitigate the distresses associated with expansive clay subgrades. Consequently, geosynthetic stabilization was adopted for reconstruction of the last section of the road (Section C3).

TxDOT PMIS database was used to evaluate the development of longitudinal cracks in the three test sections and the results are presented in Figure 17. The horizontal axis in this figure corresponds to the time from the end of construction while the vertical axis shows the LCI values. Significantly higher LCI values were observed over time in test Section C1 compared to those in test Sections C2 and C3. For example, 10 years after construction, the LCI value for Section C1 (control) was 120 while this value for Section C2 (geosynthetic-stabilized) was only 30.

Field testing and a comprehensive site condition survey were conducted between 2010 and 2012 to evaluate the performance of the different sections in FM734 (Dessouky *et al.* 2012). Section C1 showed severe longitudinal cracking and poor ride quality, while Sections C2 and C3 presented only minor surface cracking. FWD and DCP tests were also conducted on Sections C1 and C2 to characterize the pavement layer moduli. Table 4 summarizes the pavement layer moduli, as obtained from back calculations of FWD data and from correlations with DCP test data. Evaluation of the data presented in this table indicates that the moduli obtained through FWD and DCP were reasonably similar for the subgrade layer, but somewhat different for the base course layer. However, inspection of both data sets shows that both subgrade and base course layer moduli were higher in the geosynthetic-stabilized section (Section C2) than in the control section (Section C1). Surface condition of the test sections was also evaluated using historical images. Figure 18 shows the road conditions after nine years of construction for both sections. While Section C1 showed a significantly large number of longitudinal cracks (Figure 18a), Section C2 only showed comparatively less cracking (Figure 18b) and Section C3 was found to show good conditions (Figure 18c).

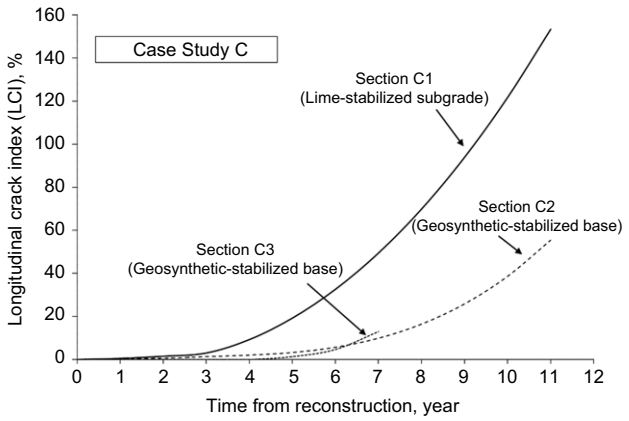

Figure 17. Longitudinal crack index (LCI) at the FM734 test sections (Case Study C)

3.4. Case Study D: SH21

3.4.1. *Site description*

Severe drop-offs at the road edge, as well as other ride quality issues, had developed from 2000 to 2010 along a portion of State Highway 21 (SH21), near Bastrop (Texas), which extends from Highway 290 to FM2440. Subgrade soils were characterized by the presence of highly expansive clays (Armstrong 2014). As part of a 2011 rehabilitation program, TxDOT constructed five test sections to assess the comparative effectiveness of different geogrids to enhance the performance of roadways founded on expansive clays. The test sections stretched from the Lee county line to approximately 3 km eastward.

The test sections involved extension of the shoulders and stabilization of the base layer in the outer lanes using five different geosynthetic products (three multiaxial and two biaxial geogrids). Figure 19 shows the extent and cross-section details of the different SH21 test sections. The original 300 mm-thick base layer in the outer lanes was excavated and replaced with a 150 mm-thick cement-treated subbase layer overlain by a new 150 mm-thick base layer. A geogrid was installed at the subbase-base interface in each test section and the shoulders were reshaped and widened by 1.5 m to provide additional lateral support to the pavement layers. Figure 20 illustrates different stages during the SH21 reconstruction.

Subgrade soil characterization results indicate Liquid Limit (LL) values ranging from 40 to 58 and Plastic Limit values ranging from 17 to 20, resulting in PI values ranging from 26 to 41 (Table 3). The subgrade soil classifies as a high plasticity clay (CH) according to the Unified Soil Classification System (USCS) (ASTM D2487-11). The specific gravity was found to be 2.784, and the optimum moisture content (ω_{opt}) and maximum dry unit weight (γ_d) were 20% and 15.42 kN/m^3, respectively (according to the standard Proctor test following ASTM D698). The average fines content of the subgrade soil was 65% while its sulfate content was negligible.

(a)

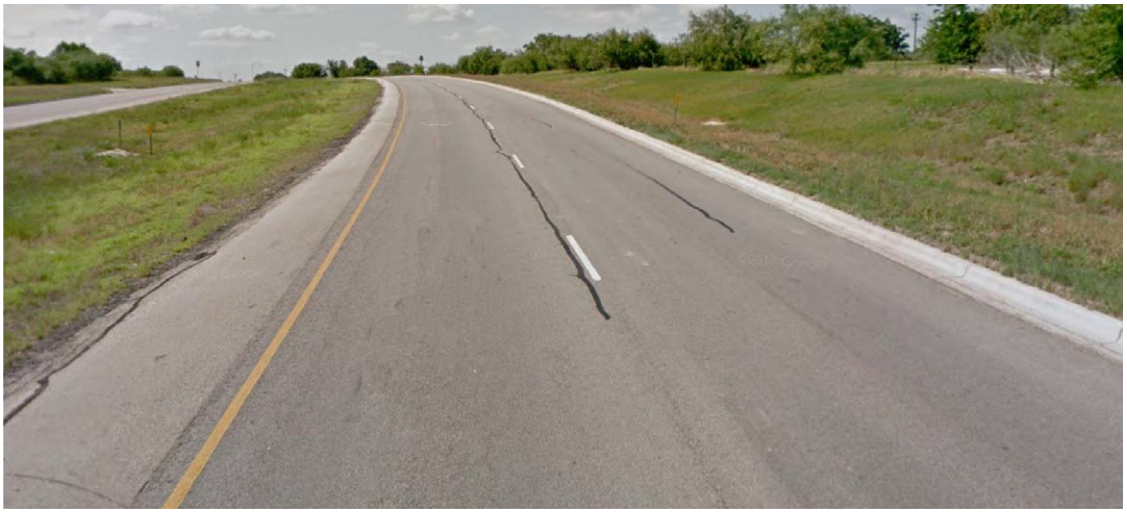

(b)

(c)

Figure 18. Road surface conditions at FM734 test sections (Case Study C) over nine years after their constructions: (a) Section C1 (control) in 2009; (b) Section C2 in 2011; (c) Section C3 in 2016

Characteristics of the geosynthetics used in the test sections are presented in Table 2. The geosynthetics used in Sections D1 and D2, GS3 and GS1, were both polypropylene, integrally-formed biaxial geogrids. The rib thickness and mechanical properties of both geogrids were similar in both machine- and cross-machine directions. However, GS1 was manufactured with rectangular apertures measuring 25×33 mm, whereas GS3 had 33 mm-long square apertures. Multiaxial geogrids GS4, GS5 and GS6 were used in Sections D5, D4 and D3, respectively. They were also integrally formed polypropylene products. The nominal rib pitch of

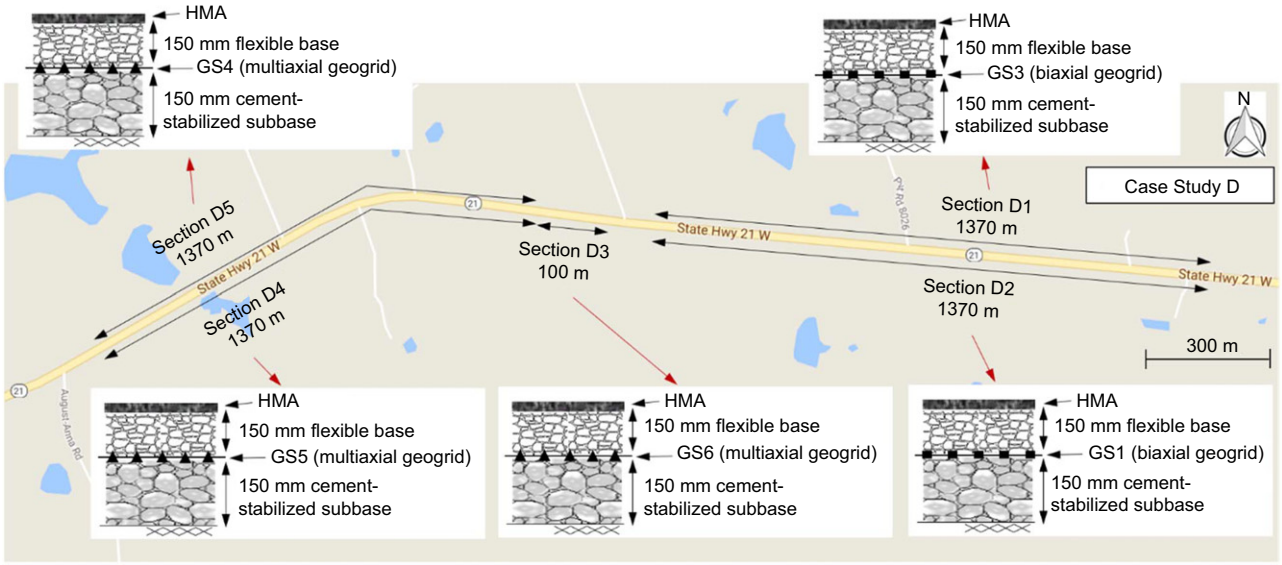

Figure 19. Layout of SH21 test sections and road profiles (Case Study D)

Figure 20. View of geosynthetic deployment during 2011 reconstruction of SH21 (Case Study D) (photos courtesy of TxDOT): (a) installation of biaxial geogrids; (b) view of old pavement layers; (c) installation of multiaxial geogrids; (d) widening of shoulders and construction of new base course

the multiaxial geogrids was 33, 40, and 40 mm for GS4, GS5, and GS6, respectively. GS6 had the largest rib and junction thicknesses among the different multiaxial geogrids.

3.4.2. *Site performance evaluation*

To evaluate the performance of the test sections along SH21, condition surveys were conducted in 2014 and 2017 to determine the extent of longitudinal cracks in each test

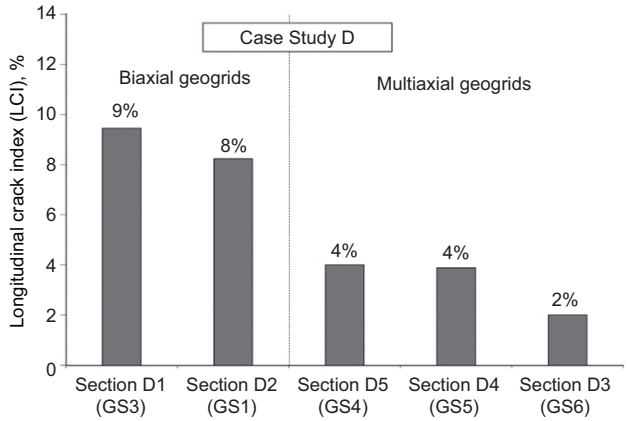

Figure 21. Comparative performance of test sections in Case Study D based on 2017 LCI in the various test sections

section. Results obtained from the 2014 condition survey indicated only minor distresses in all test sections. However, the condition survey conducted in 2017 revealed significant differences among the performances of the different test sections, particularly between those constructed using biaxial and multiaxial geogrids. LCI values obtained in the 2017 condition survey are shown in Figure 21. The test sections stabilized using multiaxial geogrids (i.e. Sections D3, D4 and D5) were found to perform better than those stabilized using biaxial geogrids (i.e. Sections D1 and D2). Specifically, while LCI was under 4% in Sections D3, D4 and D5, it exceeded 8% in Sections D1 and D2.

Among the sections stabilized using a multiaxial geogrid, Section D3, which involved the geogrid with the highest rib thickness, was found to perform comparatively better than Sections D4 and D5. Images of the roadway conditions collected in 2017 at the SH21 test sections are shown in Figure 22. Sections D5, D4 and D3, stabilized with multiaxial geogrids, are shown in Figures 22a–22c, respectively. Figure 22d shows longitudinal cracks observed in Section D2, which was stabilized using a biaxial geogrid.

3.5. Case Study E: FM2

3.5.1. *Site description*

FM2, located in Grimes County, Texas, extends for over 9 km from Courtney to FM362 (Figure 23). A 7 km portion of FM2, from State Highway 6 to FM362, had exhibited significant ride quality problems and various types of distresses, particularly in the form of longitudinal cracks. An extensive rehabilitation program was conducted to improve roadway conditions in this portion. Evaluation of cores collected from the old pavement indicated that the road profile involved a 25 mm-thick asphalt layer underlain by a 380 mm-thick base course constructed using iron ore (Figure 24). Reconstruction of the road involved scarification, remixing and compaction of the original base course to construct a 250 mm-thick subbase layer, which was subsequently overlain by a 180 mm-thick new base layer and a thin surface asphalt layer.

(a) (b) (c) (d)

Figure 22. Road conditions during 2017 survey in SH21 test sections (Case Study D): (a) Section D5; (b) Section D4; (c) Section D3; (d) Section D2

Preliminary evaluation of the subgrade soils revealed the presence of highly expansive clays. Consequently, as part of the rehabilitation program, techniques were implemented to mitigate potential damage due to the

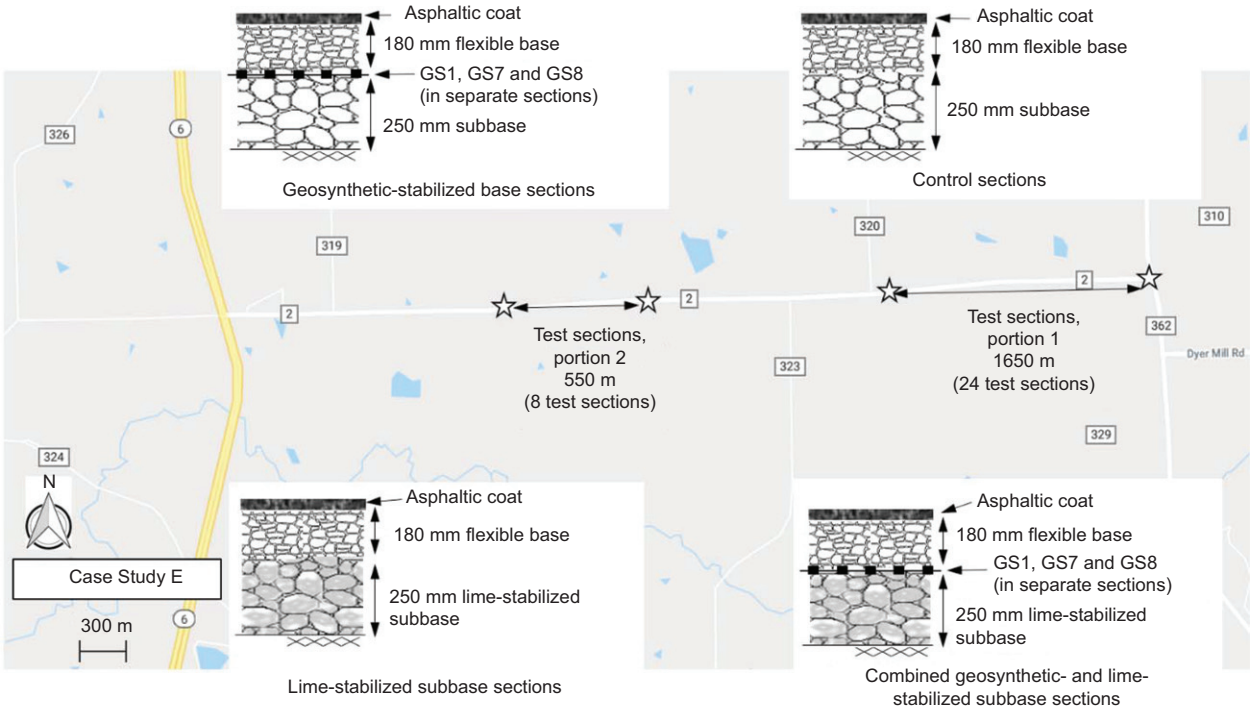

Figure 23. Layout of FM2 test sections and road profiles (Case Study E)

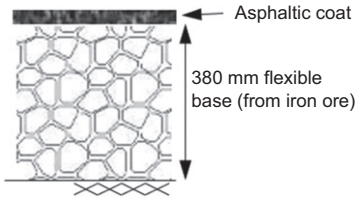

Figure 24. FM2 road profile before rehabilitation (Case Study E)

presence of an expansive clay subgrade. Specifically, the new roadway design involved chemical stabilization of the subbase (using a 4 to 6% lime dosage) and geosynthetic stabilization of the base (with a geosynthetic placed at the subbase-base interface). Ultimately, the FM2 rehabilitation project evolved into a pilot program that included a total of four different design schemes: (1) geosynthetic-stabilized base sections (using geosynthetic types GS1, GS7 and GS8); (2) lime-stabilized subbase sections (LM); (3) combined geosynthetic- and lime-stabilized sections (GS1 + LM, GS7 + LM and GS8 + LM); and (4) control sections. The various design schemes used in the FM2 test sections are depicted in Figure 23. A total of 32, 152.4 m-long test sections were constructed, involving repeats and different combinations of these four design schemes.

Subgrade soil characteristics were comprehensively investigated by collecting soil samples to a depth of approximately 2.7 m. The subgrade was mostly composed of medium to highly expansive soils, with PI values ranging from 25 to over 50. In accordance with USCS, the subgrade soils classified as CL or CH. However, sandy layers (classifying as SM or SC) were also found in some borings (Roodi 2016). The optimum water content and maximum dry unit weight of representative samples of the expansive clay subgrade were 32% and 15.5 kN/m^3, respectively (according to the standard Proctor test).

The geogrids used in the FM2 test sections were GS1 and GS7, which are biaxial geogrids with similar aperture sizes and mechanical properties in both machine and cross-machine directions. However, GS1 was a polypropylene geogrid, while GS7 was polyester. GS8 was a polypropylene woven geotextile, which exhibited a comparatively higher tensile stiffness than the two geogrids. Characteristics of the three geosynthetics used in FM2 are detailed in Table 2.

3.5.2. *Site performance evaluation*

Performance evaluation of the FM2 test sections included field assessments conducted before and after reconstruction (Roodi 2016). As part of this program, condition surveys of road surface distresses were conducted, with particular focus on quantifying the extent and severity of longitudinal cracks. The average LCI for each test section, as obtained after a severe drought that occurred 6 years after reconstruction, is presented in Figure 25. As shown in the figure, performance evaluation of the test sections indicated that the geosynthetic-stabilized sections performed considerably better than non-stabilized sections. In particular, the extent of environmental longitudinal cracks was found to be significantly lower in geosynthetic-stabilized sections than in control sections. On average, the test sections stabilized using the three geosynthetic types were found to exhibit approximately the same level of performance. In fact, while the average LCI in control sections was 65%, the average LCI in geosynthetic-stabilized sections was below 21%. These

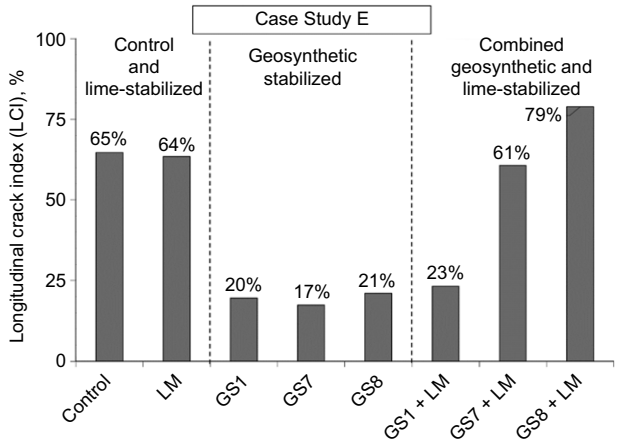

Figure 25. Comparative performance of FM2 test sections (Case Study E) based on 2011 LCI after a severe drought

Figure 26. View of road conditions of a control section (right) and a geosynthetic-stabilized base section (left) from 2011 condition survey conducted in FM2 test sections (Case Study E)

values for LCI result in a crack mitigation ratio (CMR) exceeding 3.0. Specifically, the CMR values obtained for sections stabilized using GS1, GS7, and GS8 were 3.3, 3.8 and 3.1, respectively.

Comparison of the LCIs in control sections versus those in the lime-stabilized sections, presented also in Figure 25, indicates that lime stabilization of the subbase was not necessarily helpful in mitigating the development of longitudinal cracks. Indeed, field data presented in this figure indicates that combination of lime treatment of subbase and geosynthetic stabilization of base was less effective than using only geosynthetics. These results are consistent with experiences within the TxDOT Austin District, which have shown that for roadways founded on expansive clay subgrades, treatments incorporating a rigid yet brittle layer (e.g. lime-stabilized layers) would not tolerate soil differential settlements, resulting in longitudinal cracks often more severe than cases where lime stabilization was not adopted (Sebesta and Scullion 2014). Therefore, mitigation techniques for roads founded over expansive clays should avoid approaches that lead to stiff, brittle performance (e.g. lime stabilization of subbase layers) and focus instead on approaches leading to comparatively ductile responses (e.g. geosynthetic-stabilized base courses). Figure 26 shows FM2 road conditions in 2011, illustrating a clear contrast between the good performance of the geosynthetic-stabilized section compared to the companion control section.

4. SYNTHESIS OF PERFORMANCE DATA FROM CASE STUDIES

The performance of roadways with geosynthetic-stabilized bases subjected to environmental loads are evaluated collectively in this section. Three case studies considered in this paper have incorporated control sections along with geosynthetic-stabilized sections (Case Studies A, C, and E), while two additional case studies have included experimental test sections constructed using geosynthetics with different characteristics (Case Studies B and D). Accordingly, while the roadway performance in different case studies could be affected by differences in soil types, traffic patterns and weather conditions, the impact of the geosynthetic used for stabilization can be singled out by normalizing the performance of stabilized sections in relation to control sections using the CMR values. In addition, comparative performance among test sections stabilized using different types of geosynthetic can be evaluated using LCI values.

Table 5 synthesizes and summarizes the main lessons learned and corresponding evidences from each case study. All case studies evaluated in this investigation provide conclusive information regarding the significant benefits of incorporating a geosynthetic-stabilized base layer in roadways founded over expansive clay subgrades in order to mitigate problems associated with volumetric changes (Table 5, Lesson 1). Although the different types of geosynthetics used in the various case studies (including geotextiles, biaxial geogrids, and multiaxial geogrids) resulted in improved performance, the level of improvement was found to depend on a number of factors, including the geosynthetic physical and mechanical properties. Among the different geosynthetic types adopted in the case studies evaluated in this paper, multiaxial geogrids were found to provide a better performance than biaxial geogrids, at least based on the case studies evaluated in this paper (Table 5, Lesson 2). This is quantified by results in Case Study D, which provides quantitative information on the LCI obtained for both multiaxial geogrids (LCI of 2 to 4) and biaxial geogrids (LCI of 8 to 9). While most of the case studies evaluated in this investigation considered geogrids for stabilization, woven geotextiles had also been adopted and, when considered, they were also found to provide enhanced performance under environmental loads. This is illustrated in Case Study E, where the CMR provided by woven geotextiles was found to be similar to that obtained using geogrids for base stabilization (Table 5, Lesson 3). While in-isolation tensile strength and in-isolation tensile stiffness had been specified at the time when the geosynthetics were selected in the projects investigated herein, these mechanical properties did not correlate

Table 5. Synthesis of data sources and lessons learned from the performances of geosynthetic-stabilized base courses in the different case studies

Lessons	Case Study A	Case Study B	Case Study C	Case Study D	Case Study E
Lesson 1: Geosynthetic stabilization of base course enhanced the performance of roadways subjected to environmental loads	✓ Stabilized with BXGG $LCI_{Control} = 33$[a] $LCI_{GS} = 16$ $LCI_{GS\_Reduced\ Base\ Thickness} = 26$	✓ Stabilized with BXGG $LCI_{GS1} = 8$ $LCI_{GS2} = 59$	✓ Stabilized with BXGG $LCI_{Lime\text{-}stabilized\ Subgrade} = 120$[b] $LCI_{GS} = 40$	✓ Stabilized with BXGG and MXGG $LCI_{MXGG} = 2–4$ $LCI_{BXGG} = 8–9$	✓ Stabilized with BXGG and WGT $LCI_{Control} = 65$ $LCI_{Lime\text{-}stabilized\ Subbase} = 64$ $LCI_{GS} = 17–21$ $LCI_{GS + Lime\text{-}stabilized\ Subbase} = 23–79$
Lesson 2: Multiaxial geogrids provided higher level of performance improvement than biaxial geogrids, at least for the site evaluated in this study.				✓ $LCI_{MXGG} = 2–4$ $LCI_{BXGG} = 8–9$	
Lesson 3: Base stabilization using woven geotextiles was also found to enhance performance under environmental loads					✓ $CMR_{GG} = 3.3–3.8$ $CMR_{GT} = 3.1$
Lesson 4: In-isolation tensile stiffness and in-isolation tensile strength of geosynthetics do not correlate directly with stabilization improvement levels		✓ $LCI_{GS1} = 8$ ($J_{CMD\ @2\%} = 330$ kN/m) $LCI_{GS2} = 59$ ($J_{CMD\ @2\%} = 500$ kN/m)			
Lesson 5: Geosynthetic-stabilized base may allow reduction in base course thickness	✓ $CMR_{Full\ Thickness} = 2.1$ $CMR_{Reduced\ Thickness} = 1.3$				
Lesson 6: Performance improvement by geosynthetic stabilization can be achieved in both low- and high-volume roads	✓ Low-volume road (ADT = 180)	✓ Low-volume road (ADT = 1100)	✓ High-volume road (ADT = 7400)	✓ High-volume road (ADT = 5300)	✓ Low-volume road (ADT = 880)
Lesson 7: Geosynthetic stabilization leads to a reduced modulus degradation rate and not necessarily to an increase in initial base modulus	✓ $\Delta M_{r\_Control} = 39\%$ $\Delta M_{r\_GS} = 6–24\%$		✓ $\left(\frac{M_{r\_GS-Stabilized}}{M_{r\_Lime-Stabilized}}\right)_{10\ years} = 1.32$		
Lesson 8: Geosynthetic stabilization of base course may be more effective than lime-stabilization of subbase or subgrade			✓ Comparison with lime-stabilized subgrade $LCI_{Lime\text{-}stabilized\ Subgrade} = 120$ $LCI_{GS} = 40$		✓ Comparison with lime-stabilized subbase $LCI_{Lime\text{-}stabilized\ Subbase} = 64$ $LCI_{GS} = 17–21$

GS, geosynthetic; GG, geogrid; GT, geotextile; BXGG, biaxial geogrid; MXGG, multiaxial geogrid; WGT, woven geotextile; CMR, crack mitigation ratio; LCI, longitudinal crack index; M_r, base course moduli; $J_{CMD\ @\ 2\%}$, in-isolation tensile modulus at 2% strain along cross machine direction; ADT, average daily traffic.
[a]LCI values in Case Study A correspond to 16 years after construction.
[b]LCI values in Case Study C correspond to 10 years after construction.

directly with the observed improvement levels. This is illustrated in Case Study B, where biaxial geogrids with similar in-isolation properties led to significantly different levels of improvement (Table 5, Lesson 4).

Performance data obtained for Case Study A showed the benefits of geosynthetic stabilization even in a test section constructed with reduced base thickness (Table 5, Lesson 5). Accordingly, and consistent with design strategies for a geosynthetic-stabilized base in roadways under traffic loads, the design of a geosynthetic-stabilized base under environmental loads can consider the benefit of an increased roadway service life (for a given base course thickness) or of a reduced base course thickness (for a given service life). For the conditions corresponding to Case Study A, the use of geosynthetic was found to be equivalent to reducing the base course thickness by 28% (see Figure 7).

Evaluation of the case studies presented in this paper also indicates that enhancement in roadway performance under environmental loads could be achieved by incorporating a geosynthetic-stabilized base to both low- (low ADT and thin HMA layer) and high-volume (high ADT and thick HMA layer) roadways (Table 5, Lesson 6). In addition, evaluation of the modulus obtained for the base course in Case Studies A and C indicates that, while geosynthetic stabilization of the base course may not necessarily show an initial increase in base modulus, the geosynthetic-stabilized layer, at least for the cases evaluated in this paper, clearly resulted in a reduction in the degradation rate of the base course modulus (Table 5, Lesson 7). Finally, comparison between the performance of the test sections over expansive clay subgrades stabilized using geosynthetics and that of test sections stabilized using lime indicated that adopting a geosynthetic-stabilized base, at least for the cases evaluated in this paper, proved more effective than both lime stabilization of the subbase (Case Study E) and lime stabilization of the subgrade (Case Study C) (Table 5, Lesson 8).

The aforementioned findings, based on observations from the actual performance of roadways with geosynthetic-stabilized base, underscore the significance of proper selection and design of geosynthetics to successfully fulfill the design objectives for such roadways. While the specifications considered at the time of construction of the roadways in the different case studies were based on in-isolation geosynthetic properties (i.e. without the interaction with soil) or on properties corresponding to ultimate conditions (e.g. tensile strength), observations from Case Study B indicates that the geosynthetic properties quantified in isolation or at ultimate state may not capture the mechanisms involved in geosynthetic-stabilized roadways and may result in inadequate performance, because such properties do not account for the need for proper shear transfer between the base course and the geosynthetic. Specifically, in Case Study B, although GS2 shows a higher tensile modulus and ultimate tensile strength than GS1 (see Table 2), the test section stabilized using GS2 performed significantly worse than the test section stabilized using GS1. Lack of a property that properly accounts for shear transfer between the base course and the geosynthetic is also relevant in the case of geosynthetic-stabilized base courses constructed to mitigate distress induced by traffic loads. The mechanical properties that govern geosynthetic-stabilized base courses for traffic and environmental loads are expected to involve a measure of the stiffness of the geosynthetic product under the confinement of soil. Recent research studies have identified a soil-geosynthetic composite property that is characterized under the confinement of soil (e.g. Roodi and Zornberg 2017; Zornberg *et al*. 2017) as well as correlations between field performance and such property (Roodi *et al*. 2018). The field data presented in this paper correspond to cases with multi-year performance history and, accordingly, to cases in which geosynthetic selection was not based on confined properties of the soil-geosynthetic composite. While the results presented in this investigation are unequivocal about the clear benefits of incorporating a geosynthetic-stabilized base to the design of roadways subjected to environmental loads, they also point to the need for continued refinement of the properties considered for geosynthetic selection in such applications.

5. CONCLUSIONS

An evaluation was conducted of the performance of five roadway projects involving multi-year field data from full-scale test sections that incorporated geosynthetic-stabilized base courses as an approach to mitigate problems associated with the presence of expansive clay subgrades. Each case study provides specific lessons learned regarding geosynthetic stabilization of the base course of flexible paved roadways. Collectively, they show that mitigation of distresses induced by environmental loads (e.g. presence of expansive clay subgrades) constitutes an additional objective to consider the use of geosynthetics in roadway projects. This adds to the already well-established objectives involving applications where geosynthetics are used to enhance the structural capacity to support traffic loads (e.g. by reducing the required base course thickness or by extending the roadway design life).

The test sections of the five field case histories presented in this investigation were subjected to actual traffic and environmental conditions. The availability of multiple geosynthetic-stabilized test sections allowed making comparisons between geosynthetic-stabilized test sections and companion control sections as well as among test sections stabilized using geosynthetics with different physical and mechanical properties. Focus of the evaluation presented in this paper is limited to sites characterized by the presence of expansive clay subgrades. In particular, the development and extent of longitudinal cracks on the pavement surface and associated degradation of the base course stiffness were evaluated. The extent of environmental longitudinal cracks in a given road section was expressed by the longitudinal crack index (LCI), which corresponds to the ratio between the total

length of longitudinal cracks in a road section and the length of that section, and by the crack mitigation ratio (CMR), defined as the ratio between the LCI in a control section and that in an equivalent geosynthetic-stabilized section. The following conclusions can be drawn from this investigation.

(1) For geosynthetic-stabilized and control sections with similar design and environmental loading conditions, the crack mitigation ratio (CMR) was identified as an index suitable to assess alternative designs involving roadways founded over expansive clay subgrades.
(2) The performance of field test sections involving geosynthetic-stabilized base courses was found to consistently exceed that of control sections, with CMR values typically exceeding 2. This indicates that the length of the environmental longitudinal cracks in control sections often exceeded by at least twice that in geosynthetic-stabilized sections (refer to Case Studies A and E).
(3) The use of geosynthetic-stabilized base courses was found to mitigate the time-dependent degradation of the base course stiffness in roads founded on expansive clays. Specifically, independent of a possible initial increase in base layer modulus due to geosynthetic stabilization, such base modulus was found to degrade at higher rates in control sections than in geosynthetic-stabilized sections (refer to Case Studies A and C).
(4) The long-term performance of paved road sections involving geosynthetic-stabilized base courses may exceed that of control paved road sections, even if the latter is constructed with a thicker base course (refer to Case Study A).
(5) Both biaxial and multiaxial geogrids, as well as geotextiles, were found to improve the performance of roadways constructed on expansive clay subgrades. At least for the cases evaluated in this paper, and among test sections stabilized with different geosynthetic types, the performance of sections stabilized using multiaxial geogrids was higher than that of sections stabilized using biaxial geogrids (refer to Case Study D). Also, the performance of sections stabilized with geotextiles was found to be equivalent to that of sections stabilized with several types of geogrids (refer to Case Study E). Evaluation of additional case studies may be necessary to generalize the trends observed in the case studies evaluated in this paper.
(6) While the specifications considered at the time of construction of the roadways in the different case studies were based on in-isolation geosynthetic properties (i.e. without the interaction with soil) or on properties corresponding to ultimate conditions (e.g. geosynthetic tensile strength), these geosynthetic properties may not account for the mechanisms involved in geosynthetic-stabilized roadways and may result in inadequate performance (refer to Case Study B). The mechanical properties that govern geosynthetic-stabilized base courses for environmental loads are expected to involve a measure of the stiffness of the geosynthetic product under the confinement of soil.
(7) The use of geosynthetic-stabilized base courses was found to improve the performance of field test sections founded on expansive clay subgrades not only in low-volume roads (refer to Case Studies A, B, and E) but also in the case of high-volume roadways that included a comparatively thick HMA surface course (refer to Case Studies C and D).
(8) At least for the cases evaluated in this paper, the use of geosynthetic-stabilized base courses was found to be more effective to mitigate the development of environmental longitudinal cracks than lime stabilization. This was the case for cases where lime was used to stabilize the subbase course (refer to Case Study E) and the subgrade soils (refer to Case Study C).

Overall, if adequately selected, designed and constructed, roadways with geosynthetic-stabilized base courses founded on expansive clays are expected to perform significantly better than equivalent roadways constructed without geosynthetics. Accordingly, the use of geosynthetics to mitigate problems associated with the presence of expansive clays constitutes a relevant application that adds to the portfolio of applications involving the use of geosynthetics to improve the performance of roadways.

ACKNOWLEDGEMENTS

The authors acknowledge the support received from the Texas Department of Transportation (TxDOT), including the relevant information provided by M. Arellano and D. Goehl. The assistance provided by L. Zheng, J.R. Phillips, R. Gupta and other team members from the University of Texas at Austin in the collection of field data is also greatly appreciated.

NOTATION

Basic SI units are given in parentheses.

ADT	average daily traffic (dimensionless)
CMR	crack mitigation ratio (dimensionless)
IRI	International Roughness Index (m/km)
J	in-isolation tensile stiffness of geosynthetic (N/m)
LCI	longitudinal crack index (dimensionless)
LL	liquid limit (dimensionless)
M_r	pavement layer moduli (N/m^2)
PI	plasticity index (dimensionless)
PL	plastic limit (dimensionless)
PVR	potential vertical rise (m)
TMI	Thornthwaite Moisture Index (dimensionless)
γ_d	dry unit weight (N/m^3)

ABBREVIATIONS

ASTM	American Society for Testing and Materials
BX	biaxial
CH	fat clay
CL	lean clay
CMD	cross machine direction
CMR	crack mitigation ratio
DCP	dynamic cone penetrometer
FM	Farm to Market
FWD	falling weight deflectometer
GG	geogrid
GS	geosynthetic
GT	geotextile
HMA	hot mix asphalt
LM	lime
MD	machine direction
MX	multiaxial
NW	nonwoven
PET	polyester
PMIS	Pavement Management Information System
PP	polypropylene
RAP	recycled asphalt pavement
SC	clayey sand
SH	state highway
TxDOT	Texas Department of Transportation
W	woven

REFERENCES

Al-Qadi, I. L., Brandon, T. L. & Bhutta, A. (1997). Geosynthetic stabilized flexible pavements. *Proceedings of Geosynthetics '97*, Long Beach, CA, USA, Industrial Fabrics Association International (IFAI), St Paul, MN, USA, vol. 2, pp. 647–662.

Al-Qadi, I. L., Tutumluer, E. & Dessouky, S. (2006). Construction and instrumentation of full-scale geogrid-reinforced flexible pavement test sections. *Proceeding of the Highway Pavements & Airfield Technology Conference*, Atlanta, GA, USA, Al-Qadi, I. L., Editor, ASCE, Reston, VA, USA, pp. 131–142.

Arguez, A., Durre, I., Applequist, S., Squires, M., Vose, R., Yin, X. & Bilotta, R. (2010). *NOAA's U.S. Climate Normals (1981–2010): Annual Normals*. National Centers for Environmental Information, U.S. Department of Commerce, Washington, DC, USA, https://doi.org/10.7289/V5PN93JP.

Armstrong, C. P. (2014). *Effect of Fabric on the Swelling of Highly Plastic Clays*, MSc thesis, The University of Texas, Austin, TX, USA.

ASTM D2487-11 *Standard Practice for Classification of Soils for Engineering Purposes (Unified Soil Classification System)*. ASTM International, West Conshohocken, PA, USA.

ASTM D698-12 *Standard Test Method for Laboratory Compaction Characteristics of Soil Using Standard Effort (12,400 ft-lbf/ft^3 (600 kN-m/m^3))*. ASTM International, West Conshohocken, PA, USA.

Berg, R. R., Christopher, B. R. & Perkins, S. W. (2000). *Geosynthetic Reinforcement of the Aggregate Base/Subbase Courses of Pavement Structures* GMA White Paper II, Geosynthetic Materials Association, Roseville, MN, USA.

Chen, D. H. (2007). Field and lab investigations of prematurely cracking pavements. *Journal of Performance of Constructed Facilities*, **21**, No. 4, 293–301.

Chen, Q., Hanandeh, S., Abu-Farsakh, M. & Mohammad, L. (2018). Performance evaluation of full-scale geosynthetic reinforced flexible pavement. *Geosynthetics International*, **25**, No. 1, 26–36.

Christopher, B. R., Schwartz, C. & Boudeau, R. (2006). *Geotechnical Aspects of Pavements*. Federal Highway Administration (FHWA), Washington, DC, USA, FHWA NHI-05-037.

Cuelho, E., Perkins, S. & Morris, Z. (2014). *Relative Operational Performance of Geosynthetics Used as Subgrade Stabilization*, Report FHWA/MT-14-002/7712-251. Western Transportation Institute, Montana State University – Bozeman, Bozeman, MT, USA.

Dessouky, S., Oh, J. H., Yang, M., Ilias, M., Lee, S. I., Freeman, T., Bourland, M. & Jao, M. (2012). *Pavement Repair Strategies for Selected Distresses in FM Roadways*. Texas Department of Transportation, Austin, TX, USA, Report no. FHWA/TX-11/0-6589-1.

Fannin, R. J. & Sigurdsson, O. (1996). Field observations on stabilization of unpaved roads with geosynthetics. *Journal of Geotechnical Engineering*, **122**, No. 7, 544–553.

Haliburton, T. A., Lawmaster, J. D. & McGuffey, V. C. (1981). *Use of Engineering Fabrics in Transportation Related Applications*. Federal Highway Administration (FHWA), Washington, DC, USA, FHWA DTFH61-80-C-00094.

Imjai, T., Pilakoutas, K. & Guadagnini, M. (2019). Performance of geosynthetic-reinforced flexible pavements in full-scale field trials. *Geotextiles and Geomembranes*, **47**, No. 2, 217–229.

Larkin, T. J. & Bomar, G. W. (1983). *Climatic Atlas of Texas. Texas Department of Water Resources*. Texas Department of Water Resources, Austin, TX, USA, LP-192.

Olive, W., Chleborad, A., Frahme, C., Shlocker, J., Schneider, R. & Schuster, R. (1989). *Swelling Clays Map of the Conterminous United States*. U.S. Geological Survey (USGS), Denver, CO, USA, USGS Miscellaneous Investigations Series, Map I-1940.

O'Neill, M. W. & Poormoayed, N. (1980). Methodology for foundations on expansive clays. *ASCE Journal of the Geotechnical Engineering Division*, **106**, No. GTl2, 1345–1368.

Perkins, S. W. & Ismeik, M. (1997a). A synthesis and evaluation of geosynthetic reinforced base course layers in flexible pavements: Part I experimental work. *Geosynthetics International*, **4**, No. 6, 549–604.

Perkins, S. W. & Ismeik, M. (1997b). A synthesis and evaluation of geosynthetic reinforced base course layers in flexible pavements: Part II analytical work. *Geosynthetics International*, **4**, No. 6, 605–621.

Petry, T. M. & Little, D. N. (2002). Review of stabilization of clays and expansive soils in pavements and lightly loaded structure. *Journal of Materials in Civil Engineering*, **14**, No. 6, 447–460.

Roodi, G. H. (2016). *Analytical, Experimental, and Field Evaluations of Soil-Geosynthetic Interaction Under Small Displacements*, PhD dissertation, The University of Texas, Austin, TX, USA.

Roodi, G. H. & Zornberg, J. G. (2012). Effect of geosynthetic reinforcements on mitigation of environmentally induced cracks in pavements. *Proceeding of EuroGeo5: 5th European Geosynthetics Conference*, Valencia, Spain. R. B. Servicios Editoriales, Madrid, Spain, pp. 611–616.

Roodi, G. H. & Zornberg, J. G. (2017). Stiffness of soil-geosynthetic composite under small displacements: II. Experimental evaluation. *Journal of Geotechnical & Geoenvironmental Engineering*, **143**, No. 10, 1–17, https://doi.org/10.1061/(ASCE)GT.1943-5606.0001769.

Roodi, G. H. & Zornberg, J. G. (2020). Long-term field evaluation of a geosynthetic-stabilized roadway founded on expansive clays. *Journal of Geotechnical & Geoenvironmental Engineering*, **146**, No. 4, 1–17, https://doi.org/10.1061/(ASCE)GT.1943-5606.0002206.

Roodi, G. H., Zornberg, J. G., Aboelwafa, M. M., Phillips, J. R., Zheng, L. & Martinez, J. (2018). *Soil-Geosynthetic Interaction Test to Develop Specifications for Geosynthetic-Stabilized Roadways*, Rep. No. FHWA/TX-18/5-4829-03-R1, Texas DOT, Austin, TX, USA.

Scullion, T. (2004). MODULUS 6.0. Product 0-1869-P4, Texas Transportation Institute, College Station, TX, USA.

Sebesta, S. & Scullion, T. (2014). *Developing Guidelines for Repairing Severe Edge Failures*, Report No. FHWA/TX-14/0-6271-2-1. Texas Department of Transportation, Austin, TX, USA.

Sprague, C. J. & Sprague, J. E. (2016). Full-scale trafficking of geosynthetic-reinforced road sections. *Proceeding of 3rd*

Pan-American Conference on Geosynthetics, Miami Beach, FL, USA. Industrial Fabrics Association International (IFAI), St Paul, MN, USA, pp. 1992–2001.

Tang, X., Abu-Farsakh, M., Hanandeh, S. & Chen, Q. (2014). Use of geosynthetics for reinforcing/stabilizing unpaved roads under full-scale truck axle loads. *Proceeding of the Shale Energy Engineering Conference*, Pittsburgh, PA, USA, Meehan C. L., VanBriesen J. M., Vahedifard F., Yu X. and Quiroga C., Editors, ASCE, Reston, VA, USA, pp. 591–602.

Thornthwaite, C. W. (1948). An approach toward a rational classification of climate. *The Geographical Review*, **38**, No. 1, 55–94.

TxDOT (Texas Department of Transportation) (2010). DMS-6270: Biaxial Geogrid for Environmental Cracking. Texas Department of Transportation, Departmental Material Specification 6270, Austin, TX, USA.

TxDOT (2014). *Test Procedure for Determining Potential Vertical Rise*. Tex-124-E, Texas DOT, Austin, TX, USA.

Zornberg, J. G. (2017a). Functions and applications of geosynthetics in roadways: Part 1. *Geosynthetics, Industrial Fabrics Association International*, February, **35**, No. 1, 34–40.

Zornberg, J. G. (2017b). Functions and applications of geosynthetics in roadways: Part 2. *Geosynthetics, Industrial Fabrics Association International*, April, **35**, No. 2, 34–40.

Zornberg, J. G., Gupta, R., Prozzi, J. A. & Goehl, D. (2008a). Case histories on geogrid-reinforced pavements to mitigate problems associated with expansive subgrade soils. *Proceedings of GeoAmericas 2008*, Cancun, Mexico. Industrial Fabrics Association International (IFAI), St Paul, MN, USA, pp. 983–991.

Zornberg, J. G., Prozzi, J. A., Gupta, R., Luo, R., McCartney, J. S., Ferreira, J. Z. & Nogueira, C. (2008b). *Validating Mechanisms in Geosynthetic Reinforced Pavements. Center for Transportation Research (CTR)*, Report No. 0-4829-1, Texas Department of Transportation, Austin, TX, USA.

Zornberg, J. G., Roodi, G. H. & Gupta, R. (2017). Stiffness of soil-geosynthetic composite under small displacements: I. Model development. *Journal of Geotechnical and Geoenvironmental Engineering*, **143**, No. 10, 1–13, https://doi.org/10.1061/(ASCE)GT.1943-5606.0001768.

Zornberg, J. G., Ferreira, J. A. Z., Gupta, R., Joshi, R. V. & Roodi, G. H. (2012a). *Geosynthetic-Reinforced Unbound Base Courses: Quantification of the Reinforcement Benefits*, Oakland, CA, USA. Hryciw, R. D., Athanasopoulos-Zekkos, A. and Yesiller, N., Editors. ASCE, Reston, VA, USA, Report No. FHWA/TX-10/5-4829-1. Center for Transportation Research (CTR), Austin, TX, USA.

Zornberg, J. G., Roodi, G. H., Ferreira, J. & Gupta, R. (2012b). Monitoring performance of geosynthetic-reinforced and lime-treated low-volume roads under traffic loading and environmental conditions. *Proceeding of Geo-Congress 2012: State of the Art and Practice in Geotechnical Engineering*, Oakland, CA, USA, Hryciw, R. D., Athanasopoulos-Zekkos, A. and Yesiller, N., Editors, ASCE, Reston, VA, USA.

The Editor welcomes discussion on all papers published in Geosynthetics International. Please email your contribution to discussion@geosynthetics-international.com by 15 December 2021.